Grid Integration Issues of Distributed Generations

Thesis submitted in partial fulfillment of the requirements for the degree of

Master of Technology

in

Electrical Engineering

(Specialization: Control & Automation)

by

Anupam Deori

Department of Electrical Engineering
National Institute of Technology Rourkela
Rourkela, Odisha, 769008, India

May 2015

Grid Integration Issues of Distributed Generations

Dissertation submitted in

in May 2015

to the department of

Electrical Engineering

of

National Institute of Technology Rourkela

in partial fulfillment of the requirements for the degree of

Master of Technology

by

Anupam Deori

(Roll 213EE3302)

under the supervision of

Prof. Pravat Kumar Ray

Department of Electrical Engineering
National Institute of Technology Rourkela
Rourkela, Odisha, 769008, India

Department of Electrical Engineering
National Institute of Technology Rourkela
Rourkela-769008, Odisha, India.

Certificate

This is to certify that the work in the thesis entitled ***Grid Integration Issues of Distributed Generations*** by ***Anupam Deori*** is a record of an original research work carried out by him under my supervision and guidance in partial fulfillment of the requirements for the award of the degree of Master of Technology with the specialization of **Control** & **Automation** in the department of **Electrical Engineering**, National Institute of Technology Rourkela. Neither this thesis nor any part of it has been submitted for any degree or academic award elsewhere.

Place: NIT Rourkela
Date: May 2015

Prof. Pravat Kumar Ray
Professor, EE Department
NIT Rourkela, Odisha

Acknowledgment

First and Foremost, I would like to express my sincere gratitude towards my supervisior Prof. Pravat Kumar Ray for his advice during my project work. He has constantly encouraged me to remain focused on achieving my goal. His observations and comments helped me to establish the overall direction of the research and to move forward with investigation in depth. He has helped me greatly and been a source of knowledge.

I extend my thanks to our HOD, Prof. A.K Panda and to all the professors of the department for their support and encouragement.

I am really thankful to Soumya sir and research scholars' electrical engineering who helped me during my course work. Also I would like to thanks my all friends particularly Amit, Rahul, Ankit, Sudipta and Abhilash for their personal and moral support and also for helping me in writing the thesis. My sincere thanks to everyone who has provided me with kind words, a welcome ear, new ideas, useful criticism, or their invaluable time, I am truly indebted.

I must acknowledge the academic resources that I have got from NIT Rourkela. I would like to thank administrative and technical staff members of the Department who have been kind enough to advise and help in their respective roles.

Last, but not the least, I would like to acknowledge the love, support and motivation I recieved from my parents and therefore I dedicate this thesis to my family.

Anupam Deori
213EE3302

Abstract

Paucity in the energy scenario had made conservation of energy an essential issue. Usage of Renewable energy sources (RES) is increasing in the present era, which calls for green and clean energy sources. RES includes various forms viz., solar energy, wind energy, geothermal energy etc. but the most favored are the solar and wind energy. Most RES are intermittent in nature. To integrate RES to a utility grid is a quite challenging task, to track the maximum power point (MPP) of a consistently irradiated PV system is important and is yet another challenge. Of all the available methods in the MPPT context the Perturb and observe (P & O) method and incremental conductance method are the widely used techniques. In this project the P & O method is implemented for tracking the MPP.

The tracking system conventionally is supplied the PV array voltage and current to track the MPP. In this thesis instead of having a sensor for measurement of the solar array current, it is estimated or observed with a sliding mode observer. The observer is based on sliding-mode and is constructed from the dynamic equations of the considered system viz. a single phase grid connected Photovoltaic system that has a Photovoltaic module and a single-phase H-bridge inverter. The solar array current is observed by the known values or measured values of the array voltage and inductor current. The current estimation is governed by the sliding mode observer gain, as we increase the value of the gain chattering problems come into being. The estimated value almost follows the original current and hence, is used to track the MPP. In this thesis at first the methodology of grid integration of distributed Photovoltaic systems are studied and simulated. And then an observer based on sliding-mode theory, the MPPT control was developed.

Contents

List of Figures

List of Abbreviations

AC	:	Alternating Current
BJT	:	Bi-polar Junction Transistor
DC	:	Direct Current
DG	:	Distributed Generation
F	:	Farad
FET	:	Field-effect Transistor
H	:	Henry
Hz	:	Hertz
INC	:	Incremental Conductance
IGBT	:	Insulated Gate Bi-polar Transistor
MPP	:	Maximum Power Point
MOSFET	:	Metal Oxide Semiconductor Field Effect Transistor
P&O	:	Perturb and observe
PI	:	Proportional-Integral
PLL	:	Phase Lock Loop
PV	:	Photovoltaic
RES	:	Renewable Energy Resources
SMO	:	Sliding Mode Observer

Chapter 1

Introduction

Chapter 1

Introduction

Electrical energy that is distributed or connected to the grid from many decentralized locations, viz. wind farms and PV panels is known as distributed generations. Paucity of most sources, depletion of fossils and threat to the environment has led us to the choice of switching to renewable energy sources (RES). It is not only abundant in its availability but is also pollution free and eco- friendly. Most of these energies are intermittent in nature, this makes it interesting and intriguing to connect RES into the grid. Solar energy, wind energy and geothermal energy are some of the most booming renewable energy forms.

They are everywhere around us but they cant be used in their direct form. In this thesis PV systems are taken into account. For PV systems it is very important to track its maximum power point (MPP). A tracking strategy called the maximum power point tracking comes into play for keeping track of the MPP of a PV array. There are many MPPT techniques but the most common ones are incremental conductance (INC) and Perturb and observe (P and O) MPP tracking. Here in this thesis perturb and observe technique is used to track the MPP. In order to connect the PV system to the grid it is necessary to invert the solar DC power into AC. Hence, power stages come into being for converting DC into AC. Various topologies such as the single phase H-inverter are discussed in this thesis. An observer based on sliding mode is used to estimate the solar array current, which is fed to the MPPT for tracking the MPP of the PV array.

1.1 Background

The increasing demand of non-conventional energy has made it an intriguing challenge to use this kind of energy at its best. The depletion of fossil fuels and environmental hazards are yet another reason for mankind to switch to a better option such as Renewable energy sources. Since the last decade Photo-voltaic systems has been a necessary install for commercial and domestic usage. The best part of PV based systems is its Eco-friendly and pollution free nature. Although the initial investment on its installation is a bit high but has got no match to the after benefits.

As most of the renewable energies are intermittent in nature it is therefore very important to extract the maximum usable power. Photovoltaic cells have non-linear output characteristics because of the irregularity in the incident sun rays and thus calls for an effective system to keep track of the maximum operating point or the maximum power point. The tracking system is called as the maximum power point tracking system, to this day there are various MPPT algorithms of which two methods i.e. the perturb and observe and the incremental conductance are widely used.

The tracking system based on Perturb and observe approach takes the PV array current and voltage as its inputs and calculates the power slope according to which a reference voltage is generated. Practically current sensors are required to measure the current of the solar array current which is then required to be sent to the tracker. As the installation expenses are initially high it would be better if one could reduce other expenses related to the whole configuration, instead of measuring the solar array current if we estimate the value of the current which is required to track the maximum power would withdraw the cost of current sensor.

An estimation of the PV array current based on sliding-mode is presented in this thesis. The observed value is almost the same as the actual value and can

be used to track the maximum power point (MPP). The output of the tracker is then used to generate the necessary control signals of the inverter. The various limitations associated with the observer is further discussed in this writing.

1.2 Literature Review

For carrying out the experiment successfully, reference of many available literature has been taken. Right from understanding distributed generations (DG) and grid integration, PV array design, variable structure systems etc. In the paper [1] definitions related to distribute generations are described. It emphasizes on distributed generation and its history, it also elaborates about the distribution devices such as switches, overhead capacitors for power factor improvement, fuses and lightning arresters etc. The issues and challenges associated with grid integration of renewable energy sources (RES) are proposed by [2]; this paper also states some of the possible solutions to the challenges encountered in grid integration of distributed generations. The effects of DG in distribution grid are studied from [3], here the aspects influenced on connecting DG units such as power quality, voltage control, protection system, and grid losses are explicated.

Although we are familiar with various RES but this thesis is mainly concerned with PV systems, the designing of PV module is described in [4] and [5]. These papers propose very easy and accurate designing methods using datasheets. In paper [5] an efficient equation is developed which results in more accurate modeling of the PV array. The various topologies available for integration of PV system to the utility grid had been proposed in [6]. The author explicates the centralized, string and multistring configurations; multilevel topologies have seemed to be of interest because of its lower harmonic waveform content.
The literature in MPPT context is described and discussed in [7]. The author has given the summary and comparison of various MPPT techniques available which is very useful for choosing a particular technique. From [8]-[10], design of stated MPPT systems, perturb and observe method and hill-climbing method etc. were

studied. Single stage energy conversion of PV energy system was studied from [11]-[12]. Having less number of power stages reduces switching losses as lesser number of semiconductor devices is used. An advanced technology, which not only boosts the low voltage of the PV array but also inverts the dc solar power into AC power to feed it to the grid is explained. Single phase grid connection of distributed PV systems are adopted from [16]-[19], an insight of various topologies with their comparisons related to integration of DG units are proposed by the author. Reviews regarding Single-phase grid integration of PV systems are presented in [18].

Paper [13] gives an introductory and intuitive understanding of sliding mode control and observer. Problem formulation for continuous time systems are described using examples, which was quite helpful in grasping the discrepancies and uncertainties encountered among the actual plant and its mathematical model of the plant which in turn led to the development of robust control methods. Sliding mode control approach is one of the robust controller designs. In [14] both continuous time sliding-mode observer and discrete-time sliding-mode observer designs are illustrated with examples. [15] Proposes a sliding mode technique based controller and observer for DC - DC converters.In [20]-[21] applications of sliding mode Variable structure systems and Variable structure observers are explicated.

1.3 Motivation

In the present era of crisis in energy, diminishing of fossil fuels and hazards caused on the environment automatically draws the attention of researchers towards the usage and benefits related to renewable energy sources. Which unlike conventional energy sources are uncontaminated and environment friendly. Popularity of distributed generations is flourishing on daily basis due to its green characteristics. However, Photo-voltaic (PV) system and wind energy systems are widely used. PV systems have got its own qualities of admiration in spite of its initial installation cost. These distributed generations are now being integrated with the utility in order to improve the power continuation. In the urge of using

the power of a PV system optimally, tracking the maximum power point of a PV system is really a vital challenge.

A special technique known as the maximum power point tracking (MPPT) is used to track the MPP. As per the available literature, it is found that of all the maximum power point tracking techniques Perturb and observe and the Incremental conductance methods are used more often. In this thesis a sliding mode observer is designed for the purpose of solar array current estimation and instead of the measured solar array current the estimated current is supplied to the MPPT controller in pursuance of tracking the MPP. The PV side system is connected to the utility through a single power stage i.e. an H-inverter.

1.4 Objective of the Thesis

The main purpose of this thesis is to estimate the solar array current of PV system. Without any sensor for solar array current measurement the proposed MPPT system is fed with the estimated solar array current instead of the measured value. The solar array current is the function of the voltage across the capacitor and the inductor current. Hence, the solar array current can be estimated from these measurable states. The voltage across the input capacitor in connection with the inverter and the inductor current are tapped and sent to the MPPT controller. Some of the salient points of this thesis are:

1. Designing a suitable PV array in MATLAB/Simulink .
2. Connecting the PV array to the grid without MPPT tracking.
3. Constructing an observer for solar array current estimation.
4. Validation of average values of estimated current and actual current of the PV array.
5. Implementation of Control circuit based on PLL for inverter switches.

6. Integration of the overall system with MPPT tracking based on sliding mode observer.

1.5 Organization of the Thesis

The thesis work has been organized as follows:

- **Chapter 2:** designing of PV module and study the behavior of its characteristics under varied environmental circumstances.
- **Chapter 3:**provides an prefatory summary of single phase inverter, choice of power devices and Pulse width modulation
- **Chapter 4:** presents an overview of grid connected Photo-voltaic systems and a very conventional simulation is performed.
- **Chapter 5:** in this chapter, sliding mode observer is designed for a single-phase inverter in order to estimate the current from the solar array for MPP tracking. It also includes the corresponding simulation results.
- **Chapter 6:** this chapter concludes the thesis and has future suggestion related to the present work.

Chapter 2

Photo-voltaic Array Modeling and Simulation

Chapter 2

Photo-voltaic array Modeling and Simulation

2.1 Modeling of Photo-voltaic module

The very fundamental unit of a solar array is the Photo-voltaic cell. A no of cells together forms a module these modules are then connected in series and/or parallel combinations, which finally results in a array. Typically a solar cell produces 2W amount of power but are modeled as per requirement of the user.

Photo-voltaic Cell

The very fundamental unit of a solar array is the Photo-voltaic cell. A no of cells together forms a module these modules are then connected in series and/or parallel combinations, which finally results in a array. Typically a solar cell produces 2W amount of power but are modeled as per requirement of the user.

Photo-voltaic Module

Power generated by a single cell is very less so, in order to increase the generated power, a collection of PV cells are connected in series and together these cells are called as a solar module or PV module.

Photo-voltaic Array

Sometimes, even solar modules do not suffice for some applications. To further improve the rating of a PV system, modules are connected in series or/and parallel to obtain a PV array.

The formation of modules and then array from a number of solar cells connected in series and parallel arrangement is shown in figure 2.1.

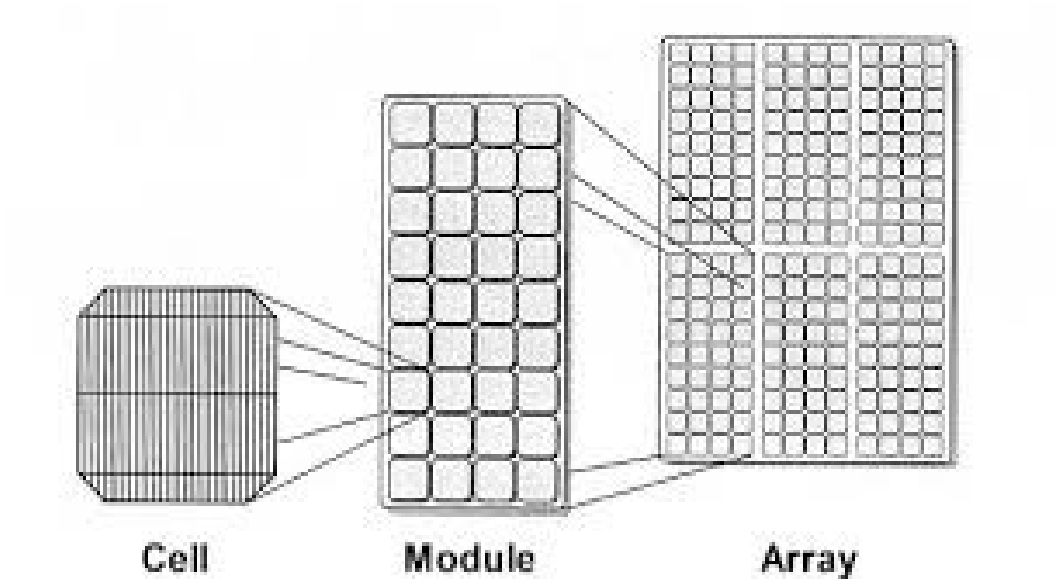

Figure 2.1: Figure showing PV cell,module and array

The electrical equivalent electrical circuit of a practical solar cell appears as in the figure 2.2. Hence, the PV cell current equation can be written as,

$$I = I_{pv} - I_d - I_p \tag{2.1}$$

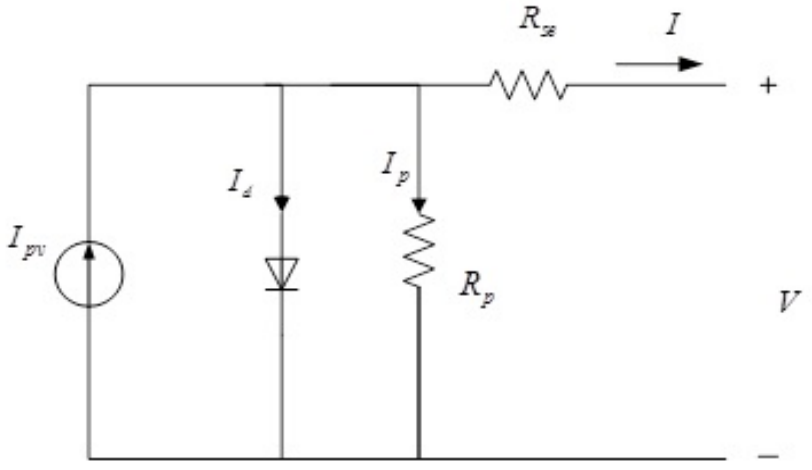

Figure 2.2: Electrical equivalent circuit of a PV cell

Where,

- $I_d = I_s(e^{\frac{q(V+IR_{se})}{nkT}} - 1)$ *and* $I_p = \frac{V+IR_se}{R_p}$

- $I_s = Reverse\ aturation\ current$
- $n = Diode\ ideal\ factor(ideal\ case = 1)$
- $q = Charge\ of\ an\ electron$
- $k = Boltzmann's\ constant$
- $T = Absolute\ temperature$

R_{se} and R_p are the parasitic series and parallel resistances of the PV cell. Decreasing the value of R_p leads in the fall of open circuit voltage of the PV cell whereas, on increasing the value of R_{se} causes the fall of the short circuit current. As aforementioned, in order to obtain a module we need to connect a group of cells in series typically,in the pursuance to improve the power and voltage of a single PV cell.The current equation for a number of cells connected in series and parallel can be written as,

$$I = N_p.I_{pv} - N_p I_s[e^{\frac{q\frac{V}{N_s}}{nkT}} - 1] \tag{2.2}$$

Where,

N_s depicts the number of cells connected in series.For improving the voltage rating of a solar module, cells are connected in series.N_p signifies the number of cells connected in parallel.likewise in order to improve the output current rating, number of cells can be connected in parallel.

2.1.1 Impact of temperature and irradiation on the parameters of a Photo-voltaic cell

$$I_{pv} = (I_{pv,N} + K_I \delta_T)\frac{G}{G_N} \tag{2.3}$$

Where,

- $I_{pv,N}$ is the current generated by incident light under nominal conditions ($25\deg\ C\ and\ 1000 Watt/m^2$)

- K_I is the temperature co-efficient of the short circuit current
- δ_T is the temperature difference of actual and nominal values (T-T_N)
- G is the light exposure or insolation
- G_N is the nominal value of insolation

The diode saturation current and its dependency on temperature can be figured from,

$$I_s = I_{s,N}.(\frac{T_N}{T})^3.e^{[\frac{qE_g}{nk}.(\frac{1}{T_N}-\frac{1}{T})]} \tag{2.4}$$

Where,

- E_g is the semiconductor band-gap energy (1.12 eV)
- k is the Boltzmann's constant ($1.3806488 \times 10^{-23}$ J/K)
- q is the elementary charge ($1.60217657 \times 10 - 19$ C)

Therefore, we can come to the culmination stating that the PV current I_pv, the diode saturation current I_s are dependent on temperature. The PV current is proportional to insolation.The value of the ideality factor of the diode n is completely factual, any initial random value of n can be chosen for the adjustment of the solar model but the convention values range between $1 - 1.4$.

2.1.2 Ratings of the solar module

The table shown below (Table 2.1) includes the parameter values for modeling of the required PV module. In this thesis KC200GT solar array is used and the respective ratings of the array are also included in the table. The following table gives the adjusted parameters of KC200GT under nominal conditions, it is to be noted that although the model is adjusted but the parameters closely resembles to the parameters of the actual model.

Table 2.1: Ratings and parameters of the used solar module

Peak power of the module	189.3 W
Voltage at max. power	26.4 V
Current max. power	7.6 A
Assured minimum peak power	185 W
I_{sc}, Short circuit current	8.21 A
V_{oc}, open circuit Voltage	32.9 V
R_{se}, series resistance	0.221 Ω
R_p, shunt resistance	415.405 Ω
K_I, temp. coefficient of I_{sc}	0.0032 A/K
K_V, temp. coefficient of V_{oc}	-0.1230 V/K
n, Diode ideality factor	1.3

2.2 Simulation results of the solar module

2.2.1 P-V characteristics

The simulation was carried out at 25^o C temperature and irradiation of 1000 W/m^2. The maximum power point which is obtained by the product of the peak values of the current and voltage of the module is highlighted in the characteristic in Figure 2.3, 189.3 W.

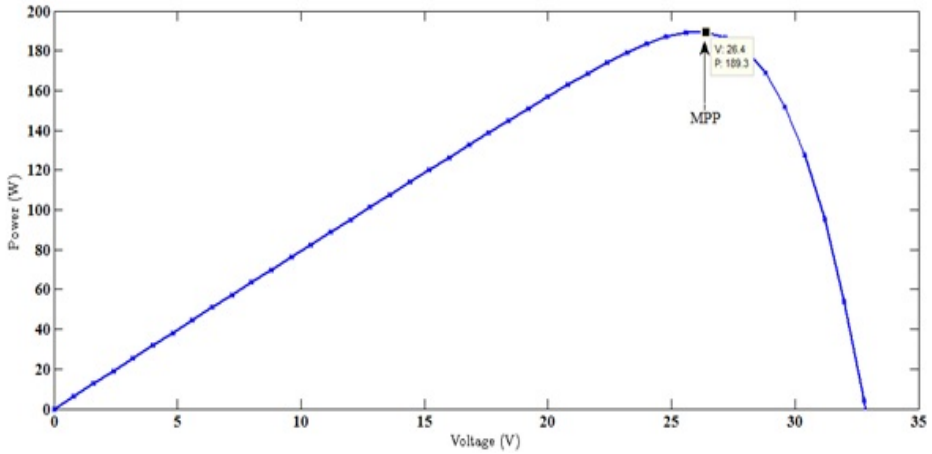

Figure 2.3: P-V characteristic of the module

2.2.2 I-V characteristics

The simulation was carried out for various insolation conditions and accordingly the behavior of the module characteristic to the variations was studied. The curve plots various voltage values for corresponding current as shown in Figure 2.4. It can be seen that the solar array short circuit current decreases as we gradually decrease the insolation. The open circuit voltage V_{oc} at the instant where solar array current I_{pv} is zero also decreases.It was further observed that on varying the temperature to higher values, the current remains almost the same but the open circuit voltage decreases as depicted in Figure 2.5.

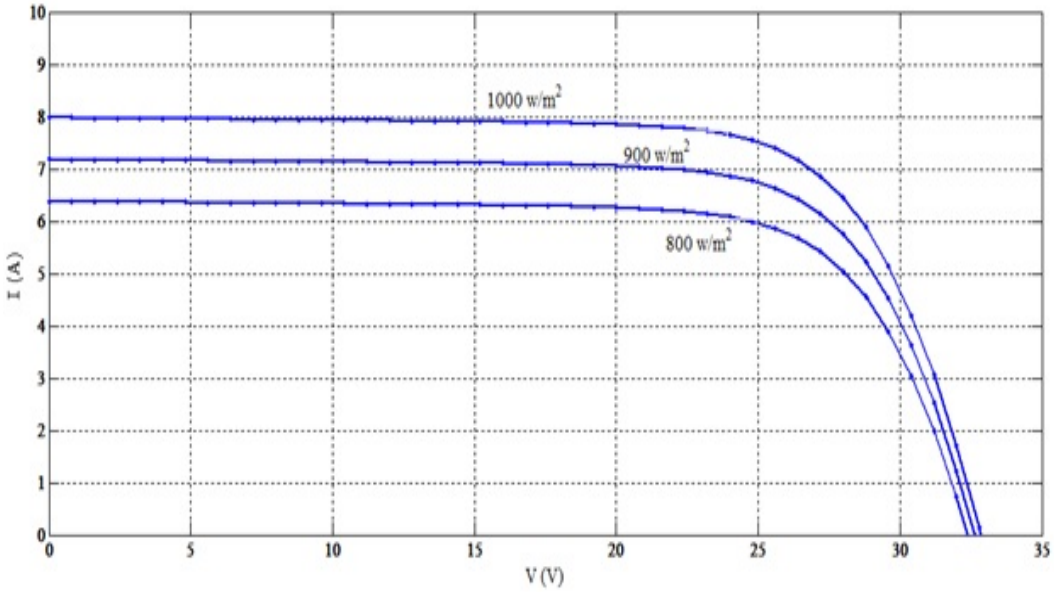

Figure 2.4: I-V characteristic of the module

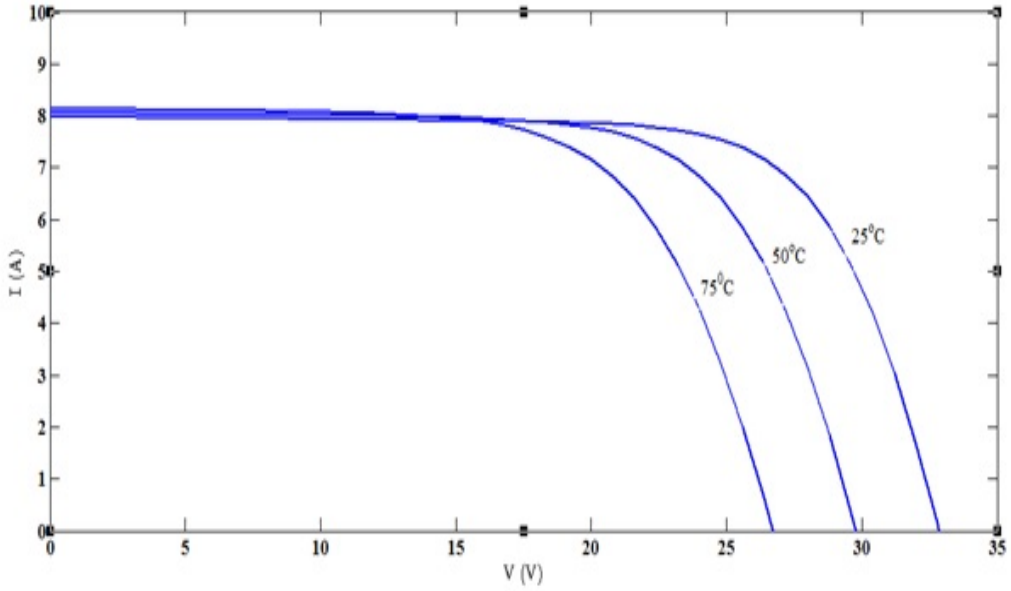

Figure 2.5: I-V characteristic of the module, Varied temperatures

Chapter 3

Single Phase Inverter

Chapter 3

Single phase Inverter

3.1 Single-phase full Bridge Inverter

Inverters are a group of power conversion circuits, which operates from DC source and converts it to symmetric AC voltage. In contrary to the converters which are used for conversion of ac power into dc, inverters works totally on the opposite principle of a converter. Usally as inputs inverters are fed with a dc source acquired from an ac source or a simple dc source.In practice, a battery bank or a PV array are the customary choices as sources for inverters. Voltage sources (magnitude) that are independent of the load are often called as stiff voltage sources. Figure 3.1 shows the circuit of a single-phase Inverter.

An ideal inverter should produce sinusoidal output waveforms but practically this is not the case, waveforms are not sinusoidal and consist of harmonics content. These inverters have one of the three waveforms at the output viz.

- Square wave
- Modified(quasi) square/sine wave
- true sinusoidal wave

The first two are acceptable for medium as well as low power applications. The modified square/sine wave inverters are slightly better than the square wave inverters in terms of their low harmonics content. The true sine wave inverters are the present day usage inverters; the waveforms yielded by these inverters are same

as that of the utility or rather better and enhanced. Harmonics also get vanished virtually in the waveforms in case of the true sine wave inverters. Varying either of the entities viz.,dc input voltage or gain of the inverter leads to the synthesis of a variable voltage (not dc in nature). Both of them are not varied at once.One of these entities is kept fixed while the other is being varied i.e either dc input is varied while the gain is kept constant or the inverter gain is varied and dc input is kept constant and so So can be realized with the use Pulse Width Modulation (PWM) control for the single phase inverter. In this method the width of the pulses of the square wave in positive as well as in the negative half in accordance to the root mean square (RMS) of the output. Ratio of the RMS ac output and the dc input represents the inverter gain.

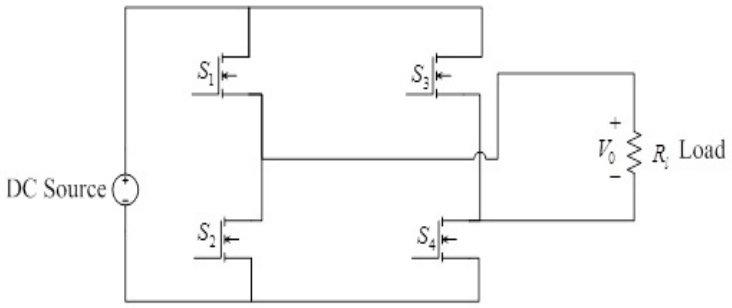

Figure 3.1: Single-phase inverter

3.1.1 Pulse Width Modulation

Various analog circuits are controlled using the pulse width modulation (PWM) technique, these analog circuits are controlled using the digital output of a processor. Applications of this technique range from measurement and communication to power conversion and control.

In order to generate control signals for the inverter switches by this method requires a reference signal, which should be a sinusoidal l signal and a carrier signal usually a triangular wave, which controls the switching frequency. These two signals are then compared to obtain the pulses. There are two methods of switching with PWM viz. Unipolar method and bipolar method of switching. In

unipolar strategy unlike bipolar method the output signal is either switched from low to zero or high to zero whereas in a bipolar method of switching the signal is switched from low to high or high to low. The switching control for a unipolar scheme is presented below:

- S_1 gets turned on when $V_{sin} > V_t$
- S_2 gets turned on when $-V_{sin} < V_t$
- S_3 gets turned on when $-V_{sin} > V_t$
- V_4 gets turned on when $V_{sin} < V_t$

An alternate strategy based on the unipolar scheme has only a pair of switches operated by the reference frequency whereas rest of the switches are operated at the frequency of carrier signal. Therefore two of the switches are low frequency switches and two of them are high frequency switches. The mentioned strategy is framed as given below:

- S_1 gets turned on when $V_{sin} > V_t$
- S_2 gets turned on when $-V_{sin} > zero$
- S_3 gets turned on when $-V_{sin} < zero$
- V_4 gets turned on when $V_{sin} < V_t$

The advantage of choosing PWM control in place of analog control is its immunity to noise and for this reason PWM is sometimes used in communications. Figure 3.2 shows the unipolar scheme.

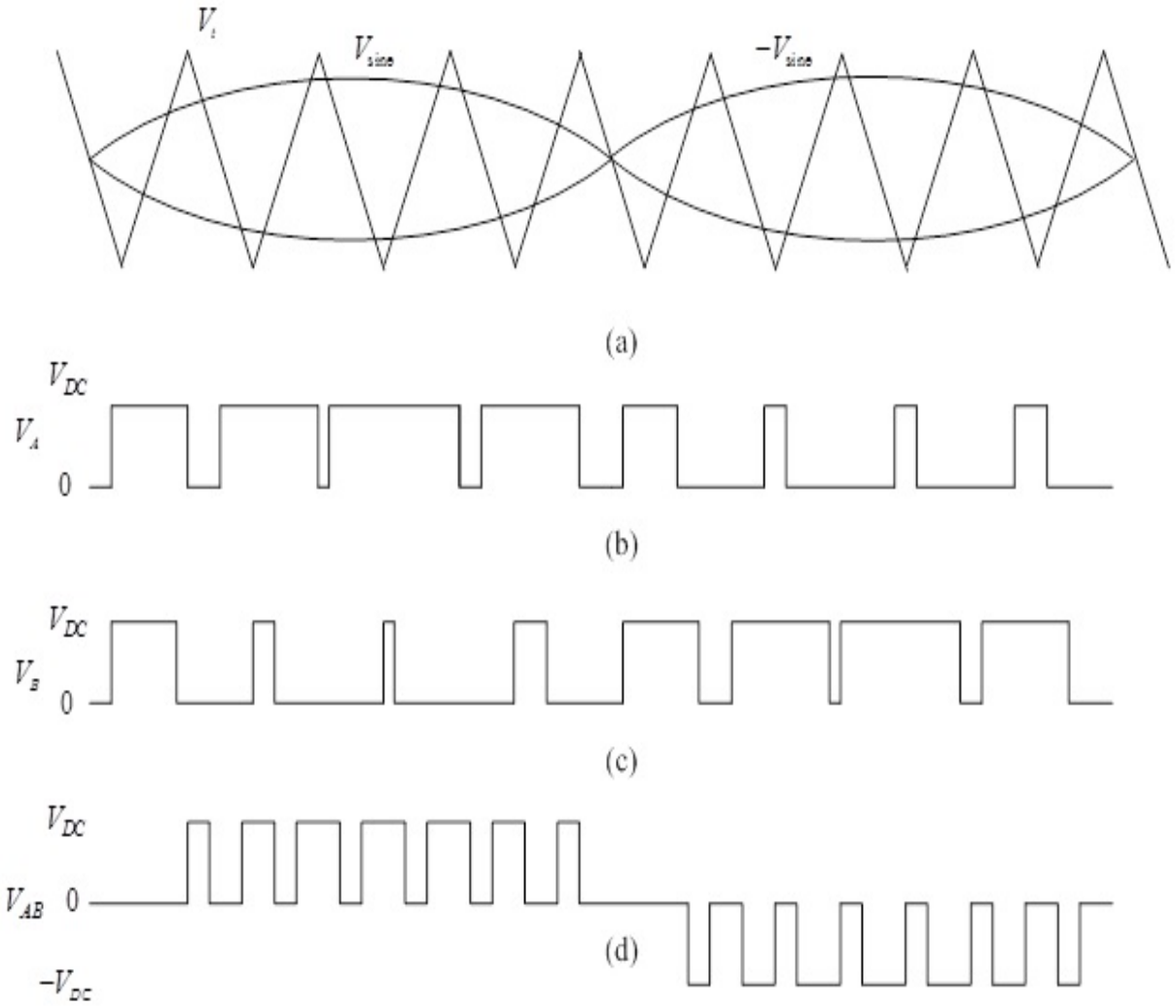

Figure 3.2: Unipolar strategy (a)carrier and reference signals (b)Voltages of the bridge (c)output voltage

3.2 Choice of Power devices

The best of conventional bipolar transistors and FETs are merged together in an Insulated Gate Bipolar transistors (IGBT). Like FETs IGBTs, only a voltage across the base is required for conduction. They are also effective conductors of current through their emitters/collectors like the conventional bipolar junction transistors (BJT).

A high base current is necessary in order to turn on a BJT, the turn-off characteristics of a BJT is relatively slow (current tail), and due to its negative temperature co-efficient it is liable for thermal runaway. To add, the conduction loss or the lowest attainable on-state voltage is controlled by the collector-emitter voltage at saturation.

However, MOSFETs are voltage controlled devices unlike BJTs. These have positive temperature coefficient, thus eliminating thermal runaway. As per theory, the on-state resistance has no restrictions. Hence, we can be further lower the on-state losses. The body to drain diode has a profound usage concerned to the limited freewheeling currents in a MOSFET.

Looking at the benefits of the IGBT its an obvious to opt for IGBT as a switching device. Having the bests of both BJT and MOSFET has made IGBT an enhanced device in the power-electronics field.

Chapter 4

Single-phase Grid Integration of Distributed Generations and simulation

Chapter 4

Single-phase Grid Integration of PV system and Simulation

4.1 Introduction

Extracting the maximum power of a PV system is a prime concern so as to feed it into the utility. So, tracking the maximum power point as well as optimization of the energy conversion are the main modeling issues for grid integration.However, power quality, synchronization with the grid, protection of the system and reliability are some of the other vital issues that require special attention while connecting PV systems to the grid. Voltage rise effect is yet another challenge which limits the integration.distributed generation (DG) units when connected to the feeder may lead to improper voltage control of the system. If the power fed to the grid by the DG units is less than or equal to the feeder load but if this is not the case voltage rise occurs as an effect of reverse power flow which gets stronger when DG interject reactive power as well; dependent on $\frac{X}{R}$ ratio. Harmonic content and transient voltage variation are the two important and usually considered aspects under power quality in general. For instance if we consider a case of a PV array exposed to an irradiation level of 600 W/m^2 and suddenly the insolation level changes to 900 W/m^2 which leads to variations in the output of the array and can lead to a voltage transient. Addition of generation and increasing the fault level of the network oftentimes improves the power quality. As far protection of DG integrated systems usually are provided with a elementary overcurrent protection strategy. Connection of DG units give rise to various sources of fault current.

False tripping, unsynchronized reclosing, prohibiting automatic reclosing are some of the identified problems associated with protection of DG connected systems. The profoundness of PV systems has made it an intriguing challenge to work out on these issues, depletion of conventional resources is another reason to switch to RES.

4.2 Topologies for grid connected PV systems

Organization of PV systems can be done in various possible ways that has direct impact on the structure as well as the topology of the converter. Conventionally the low voltage of the solar panel is boosted through a dc-dc converter and as the panel is to be connected to the utility grid it also requires a dc-ac converter or simply an inverter to convert the dc power into ac for injection into the grid. The whole configuration including the converter circuit and the panel regulates the cost,operation and its efficiency.

4.2.1 Centralized configuration

As the name suggests this topology has a central power conversion system. A multiple number of PV panels are connected together in series and parallel to form an array, this topology is suitable for PV plants having nominal power greater than 10 KW. Each string of this configuration is provided with a blocking diode to forbid energy reversal due to operation of strings at different insolation level and included energy storage systems as shown in Figure 4.1. This kind of topology are generally favored in three-phase grid connection.

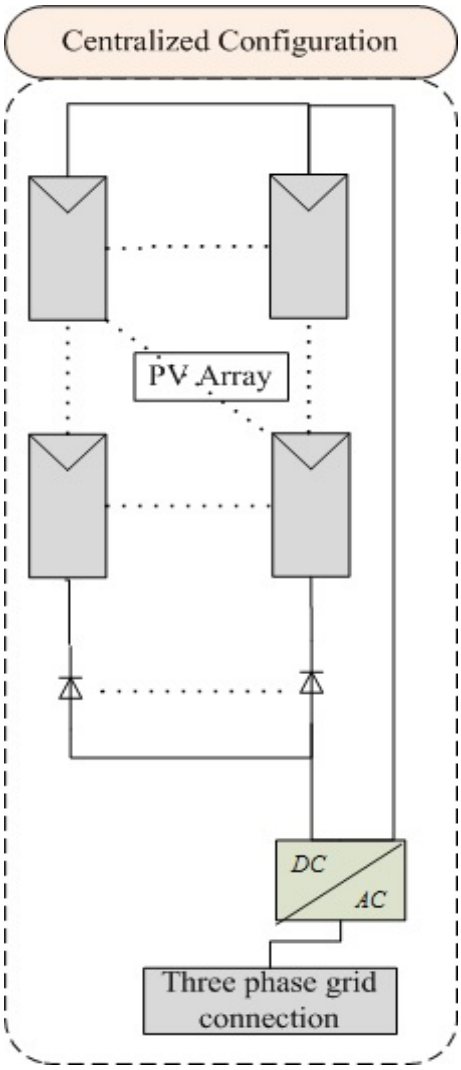

Figure 4.1: Centralized Configuration

4.2.2 String Configuration

PV panels are connected in a number of strings and each string is provided with an inverter for converting dc into ac. This topology is an easy and modified version of the centralized topology. Many a times the voltage generated by these strings are not sufficient for particular applications and needs to be boosted which is done either by a dc-dc boost converter or a step-up transformer. This topology is often implemented for single-phase integration of PV arrays and the configuration is shown in Figure 4.2.

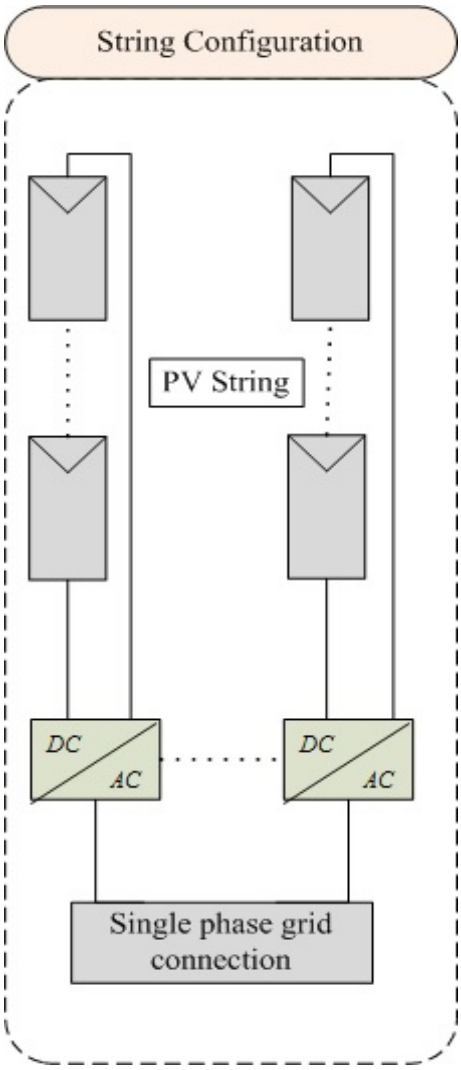

Figure 4.2: String configuration

4.2.3 Multistring Configuration

For obtaining better performance ,improving the overall plant efficiency and ease in the integration process, pros of both centralized and the string topology are merged together and the resulting configuration is called as the multistring configuration,shown in Figure 4.3. Every dc-dc converter is incorporated with a MPPT system for a specific string. Like in centralized configuration this topology also has a central dc to ac inverter besides the dc-dc converters as in string configuration.

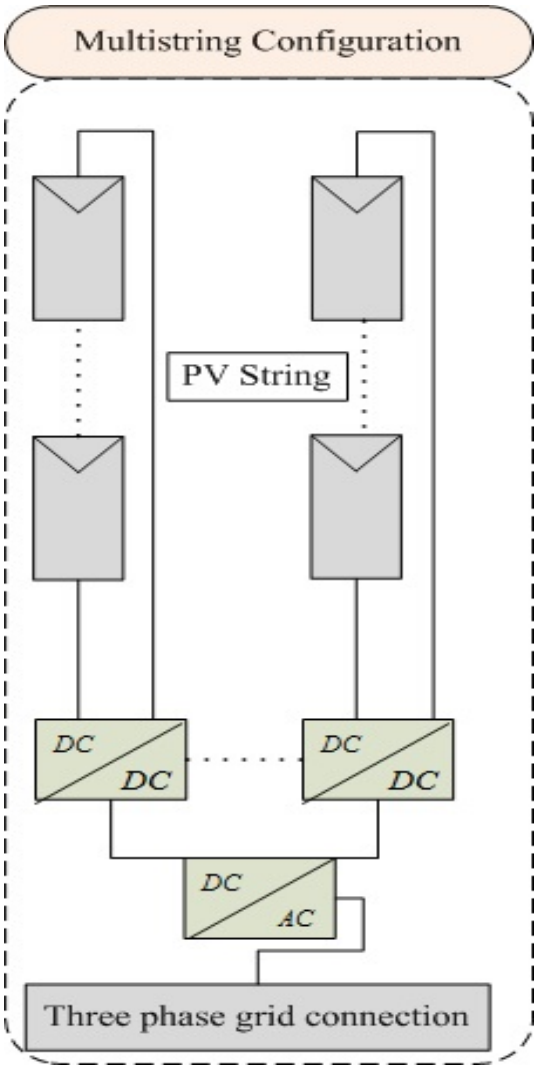

Figure 4.3: Multistring Configuration

4.2.4 AC Modules Configuration

In this configuration PV modules are connected to a dc-ac converter which performs the MPPT task automatically. This topology can be looked into as a plug-and-play system, possessing a module integrated to an inverter i.e every module has an inverter dedicated to it. Usually, the maintenance of this configuration is quite difficult in comparison to other configurations at times when the power generated by the plant increases. This scheme suits for single-phase integration with the grid, the configuration is shown in Figure 4.4

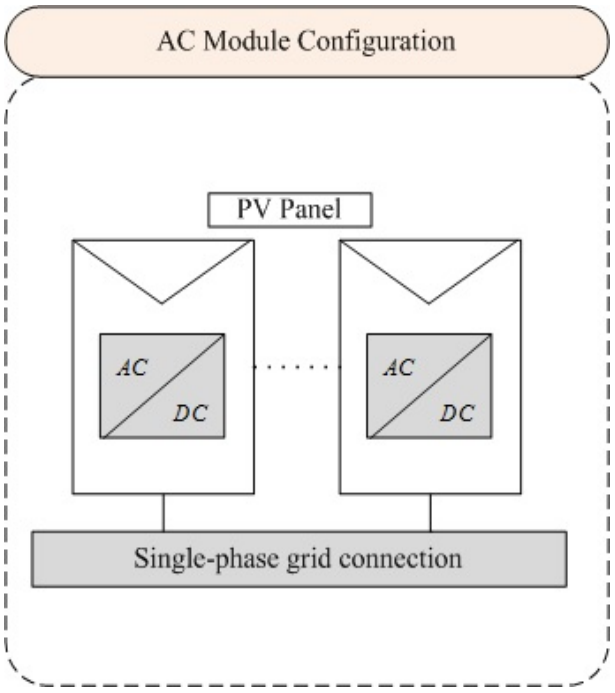

Figure 4.4: AC Modules Configuration

4.2.5 Modular Configuration

Each String of modules are connected to a dc-dc converter and shares a common dc bus with a dedicated inverter provided each dc-dc converter incorporates a MPPT system as shown in Figure 4.5. A number of inverter connections can be made as per required power level. With this type of configuration the reliability of the grid integration increases and its maintenance is also easy with the replacement of only damaged or faulty converter. The dc-dc converter adjusts the dc voltage as well as tracks the MPP. Because of the low harmonic content and reduced stressful operation of semiconductor devices of multilevel configuration, this type of configuration are widely used commercially nowadays. For completion of the integration of PV systems with the grid a suitable filters such as L,LC or LCL is needed between the dc-dc and dc-ac power stages.

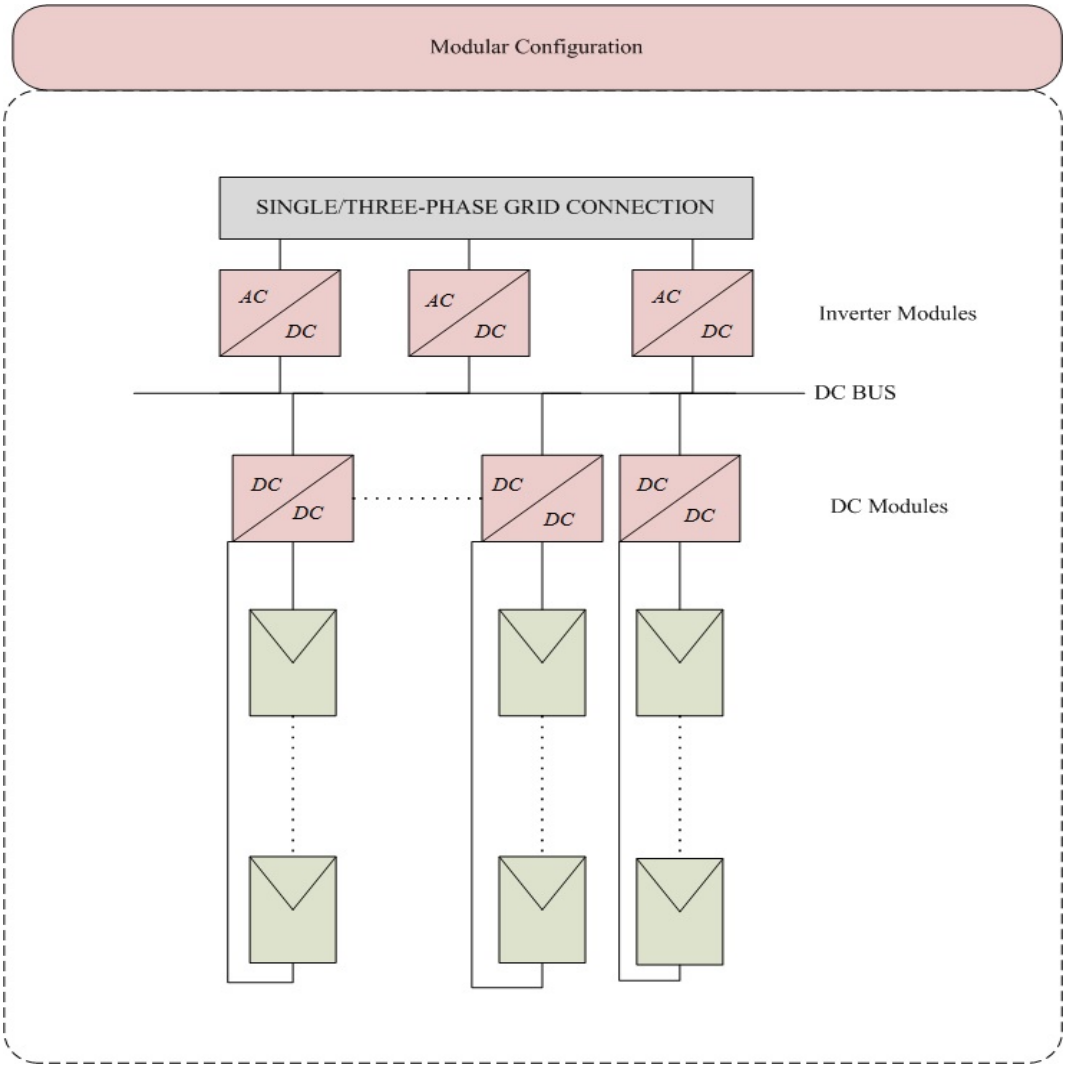

Figure 4.5: Modular Configuration

Therefore, as far the suitability and commercial requirement is concerned any of these configuration can be implemented for integration with the grid.

4.3 Simulation of single-phase grid connection of PV module

A very conventional simulation for the purpose of getting a clear picture of integration of PV array with the grid is performed. The overall configuration is shown below in Figure 4.6, the switching signals for the inverter switches were generated by implementation of hysteresis current control.

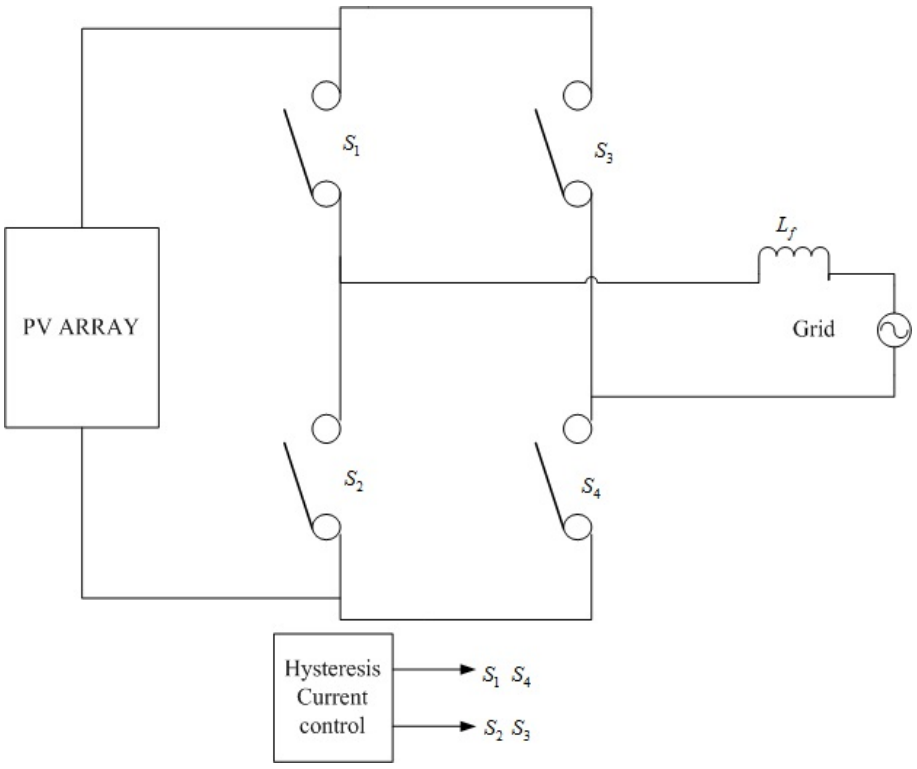

Figure 4.6: PV array integration with the grid

The grid voltage is set to a peak value of 325 volt, the PV array is considered under uniform insolation condition. The first pair S_1, S_4 are turned on for the positive half cycle and the pair S_2, S_3 is kept on for the negative half cycle. The control signals are provided using hysteresis current control method for the simulation. The voltage and current obtained during the simulation are shown in

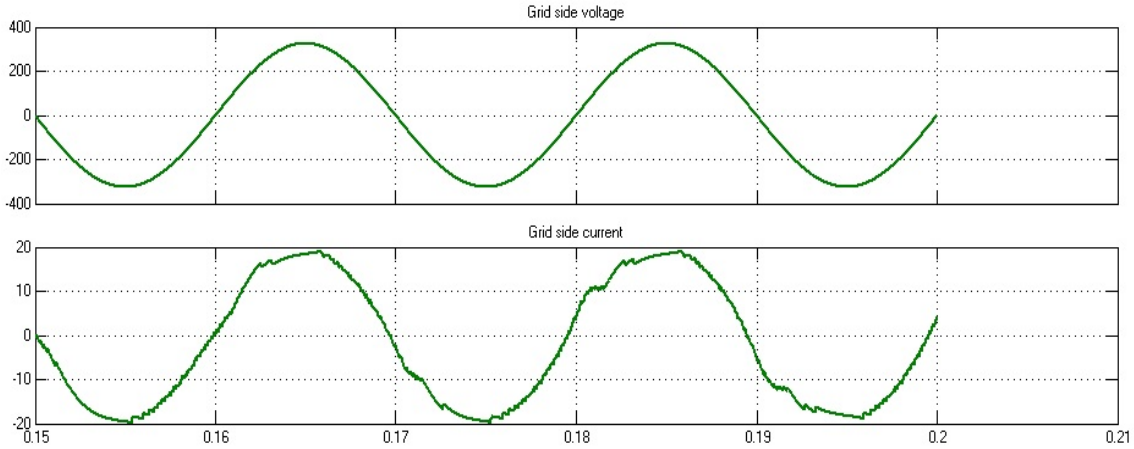

Figure 4.7: Grid voltage and grid current

Figure 4.7, It can be seen that the voltage and current are in phase, although the current has some ripple content it is nearly sinusoidal in appearance. For a better picture both the current and the voltage are shown together in Figure 4.8.

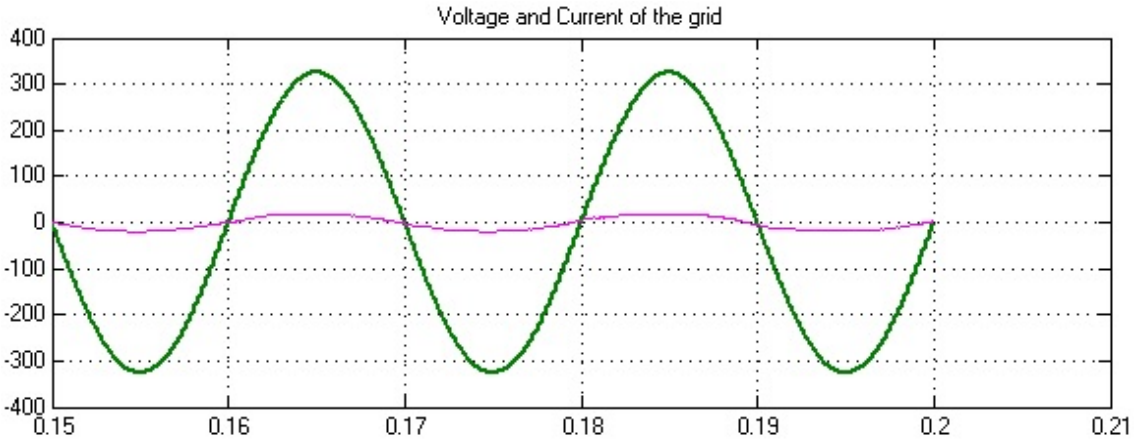

Figure 4.8: Voltage and Current of the grid

On changing the value of the inductor from $25mH$ to $10mH$ following results were obtained (Figure 4.9). Looking at the Figure 4.9 and Figure 4.8, it can be perceived that the ripple contents increase on lowering of the inductance value but the waveform remains sinusoidal and in phase with the grid voltage. Further decreasing the value to $5mH$ increases the amount of ripple content.The inductor current and grid voltage at $L = 5mH$ are shown in Figure 4.11.

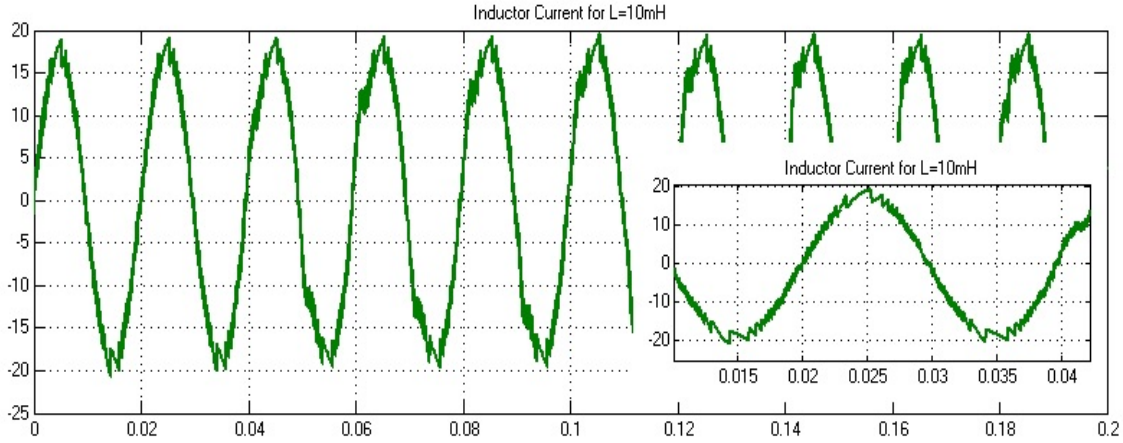

Figure 4.9: Inductor current for $L = 10mH$

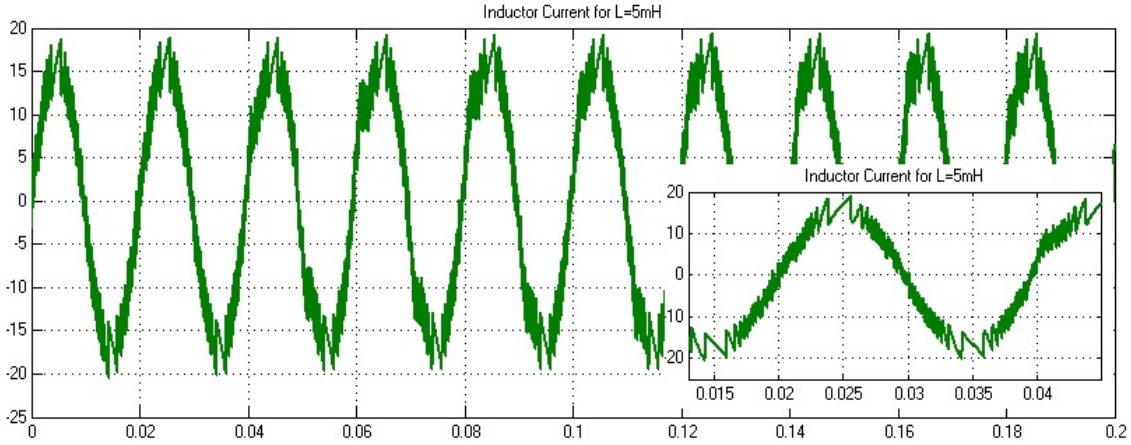

Figure 4.10: Inductor current for $L = 5mH$

Thus, a very conventional integration of the PV array was performed with the grid along with relevant simulations for better understanding. The present case considers an adjusted environment for the sake of simplicity in simulation such as the irradiation level and constant voltage.

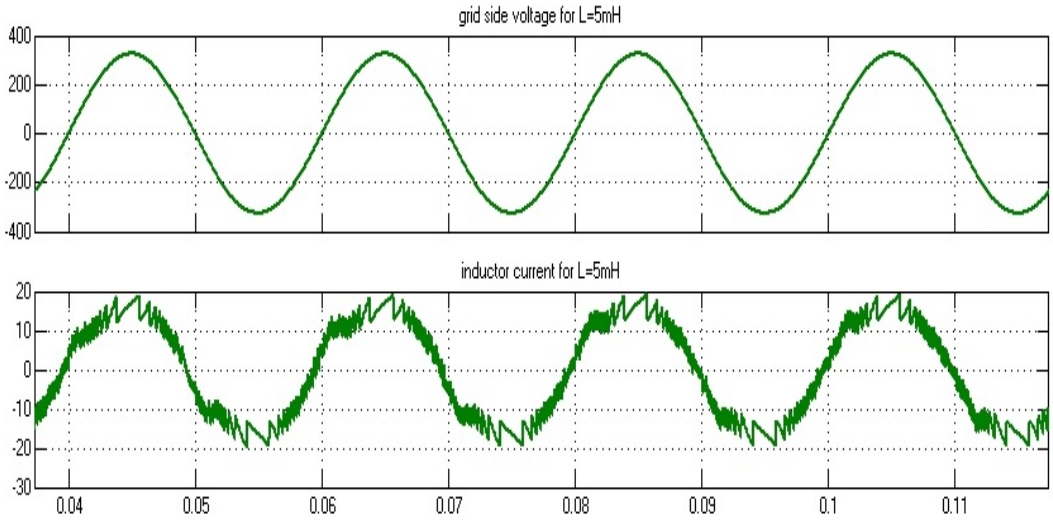

Figure 4.11: Inductor current and grid voltage for $L = 5mH$

Chapter 5

Sliding-mode Observer Design and Simulations

Chapter 5

Sliding-mode Observer Design and simulations

5.1 Observer

In the context of multivariable systems, lots of controllers are usually of the linear or non-linear state feedback type and they ask for the complete info about the states of the plant whenever they are to be implemented. However, it is either unfitting or not possible to measure all the state variables due to some limitations in practical. The solution to this very problem is to introduce an observer. An observer can be taken as an ancillary dynamic system, which is driven by the available inputs and outputs of a system yielding the original state vector with some structural supposals made on the system ensuring limitations.

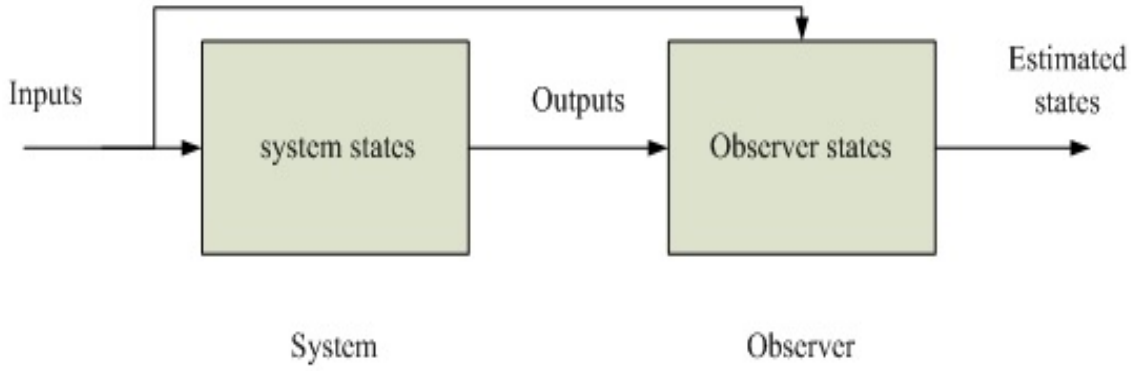

Figure 5.1: Open loop observer

5.1.1 Asymptotic Observers

Let us consider the continuous-time system,

$$\dot{X} = Ax + Bu$$
$$y = Cx \tag{5.1}$$

Where $x \in R^n$,$u \in R^p$,$y \in R^m$ and A,B and C are constant matrices of proper dimensions. These matrices are known. The pair is assumed to be observable and it is also assumed that the matrix has full rank without losing generality. The plant states are unknown; nevertheless the linear combination of the plant states forms the output vector or we can say that the output vector is a linear composition of the states of the plant and is measurable.Hence,it all narrows down to the possibility of designing a new dynamic system, which probably estimates the original state vector by just using the output and the input vectors of the system.

The standard Luenberger observer takes the following form,

$$\dot{\hat{y}} = A\hat{x} + Bu + L(y - C\hat{x}) \tag{5.2}$$

By subtracting (5.2) from (5.1) we have,

$$\dot{e} = (A - LC)e(t) \tag{5.3}$$

Here $e = x(t) - \hat{x}(t)$ depicts the difference between the actual and estimate value of the state. As it is supposed that the taken system is observable, the Eigen values of the matrix $(A - LC)$ can be so assigned such that error $e(t)$ decays to zero $e(t) \to 0$ tending to infinity i.e. $t \to \infty$. The convergence rate is determined by the Eigen values of $(A - LC)$ As per literature, this is a full order Luenberger observer as the order of the observer is equal to that of the system.Nevertheless, since there are m number of output states, transforming y should give m of the state variables directly. The transformed states are given as,

$$\begin{bmatrix} \dot{y} \\ \dot{x_1} \end{bmatrix} = \begin{bmatrix} A_{11} & A_{12} \\ A_{21} & A_{22} \end{bmatrix} \begin{bmatrix} y \\ x_1 \end{bmatrix} + \begin{bmatrix} B_1 \\ B_2 \end{bmatrix} u \tag{5.4}$$

Since y is known, there is no need to estimate it, thereby reducing the order of the observer. Now we need to reconstruct x_1 only, let the observer associated with x_1 be,

$$\dot{\hat{x_1}} = G\hat{x_1} + H_1 y + H_2 u + L\dot{y} \tag{5.5}$$

Substituting for $\hat{y}$ into (5.5) and subtracting (5.5) from (5.4) gives,

$$\dot{e_1} = Ge_1 + (A_{21} - LA_{11} - H_1)y + (A22 - g - LA_{12})x_1 + (B_2 - H_2 - LB_1)u \tag{5.6}$$

Where e_1 represents the error in x_1. G, H_1 and H_2 can be chosen as,

- $G = A_{22} - LA_{12}$
- $H_1 = A_{21} - LA_{11}$
- $H_2 = B_2 - LB_1$

It can be seen that the error dynamics associated with becomes independent of the states and the inputs of the system can be assured to decay to zero satisfying the relation:

$$\dot{e_1}(t) = (A_{22} - LA_{12})e_1(t) \tag{5.7}$$

Choosing the matrix $(A_{22} - LA_{12})$ to be stable.We further assume that the pair (A_{22}, A_{12}) is observable. Since, the pair (A, C) is observable as already stated in the beginning the pair (A_22, A_12) is observable. Hence, the Eigen values of$(A_{22} - LA_{12})$ can be randomly placed and $e_1 \to 0$ as $t \to \infty$. To discard the $\dot{y}$ term in the observer, we define a new variable:

$$\eta = \hat{x_1} - Ly \tag{5.8}$$

$$\implies \eta = (A_{22} - LA12)\eta + (A_{22}L - LA_{12}L + A_{12} - LA_{11})y + (B_2 - LB_1)u \tag{5.9}$$

and $x_1 = \dot{\eta} + Ly$ gives the the final estimate. It is to be noted that the observer has reduced to (n-m) order and asymptotic convergence takes place.

5.2 Sliding-mode Observer

We have seen that the state estimation is done asymptotically, the Eigen values related to the error dynamics can be chosen very far away from the jw-axis in the urge to increase the decay rate, however the tendency of a Luenberger observer to converge asymptotically cannot be removed totally. The same system in (5.1) is reconsidered. To at least reconstruct the states asymptotically, with only the input and output vectors of the considered system an observer can be proposed in the following manner,

$$\dot{\hat{x}} = A\hat{x} + Bu + Lsgn(y - \hat{y}) \tag{5.10}$$

$$sgn(y) = \begin{cases} +1 & y > 0 \\ -1 & y < 0 \end{cases}$$

$L \in R^{n\times m}$is the observer parameter, its value is chosen in order to attain convergence of $\hat{x}$ to x . Subtracting (5.10) from (5.1) yields,

$$\dot{e_x} = Ae_x - Lsgn(e_y) \tag{5.11}$$

e_x and e_y are the error systems, the main aim in the observer agenda is to choose the value of L in a way that $e_x \to 0$ as $t \to \infty$. Where, R is chosen randomly, $R \in R^{(n-m)\times n}$ till T invertible and $x_1 = Rx$ we get,

$$\begin{bmatrix} \dot{y} \\ \dot{x_1} \end{bmatrix} = \begin{bmatrix} A_{11} & A_{12} \\ A_{21} & A_{22} \end{bmatrix} \begin{bmatrix} y \\ x_1 \end{bmatrix} + \begin{bmatrix} B_1 \\ B_2 \end{bmatrix} u \tag{5.12}$$

Where,

$$T(A)T^{-1} = \begin{bmatrix} A_{11} & A_{12} \\ A_{21} & A_{22} \end{bmatrix}, \; T(B) = \begin{bmatrix} B_1 \\ B_2 \end{bmatrix},$$

The sliding-mode based observer for reconstruction of states of the system with this new representation is described as,

$$\begin{aligned} \dot{\hat{y}} &= A_{11}y + A_1 2x + B_1 u + L_1 sgn(e_y) \\ \dot{\hat{x_1}} &= A_{21}y + A_2 2x + B_2 u + L_2 sgn(e_y) \end{aligned} \tag{5.13}$$

Where, L_1 is a $m \times m$ matrix and L_2 is a $(n-m) \times m$ matrix. The state reconstruction error discrepancy is represented as,

$$e_y = y - \hat{y}$$
$$e_{x_1} = x_1 - \hat{x_1}$$

The error dynamics so obtained are,

$$\dot{e_y} = A_{11}e_y + A_{12}e_{x_1} - L_1 sgn(e_y)$$
$$\dot{e_{x_1}} = A_{21}e_y + A_{22}e_{x_1} - L_2 sgn(e_y) \tag{5.14}$$

Thus, reconstruction of states turns into a regulatory problem associated with e_y and e_{x_1}.The solution to this problem is the introduction of two steps of sliding-mode theory. First, maneuvering the error trajectories to a manifold defined as $S = \{e_{x_1} | e_y = 0\}$. Now let us choose a Lyapunov function for the variable e_y,

$$v = \frac{1}{2}e_y^2 \geqslant 0 \tag{5.15}$$

Considering L_1 to be a diagonal matrix where each element is greater than $\|A_{11}e_y + A_{12}e_{x_1}\|_\infty$.

$\implies \frac{dv}{dt} = e_y(A_{11}e_y + A_{12}e_{x_1} - L_1 sgn(e_y)) \leqslant 0$

The error e_y diminishes monotonically and in the end becomes zero. It is to be noted that the equality sign holds only when e_y is a zero vector. Indeed the system is asymptotically stable and L_1 ensures the asymptotic stability. As per equivalent control method substituting $e_y = 0$ and $\dot{e_y} = 0$ in the first equation of (5.14) we get,

$$(L_1 sgn(e_y))_{eq} = A_{12}e_{x_1} \tag{5.16}$$

Second equation of (5.14) can be rearranged as,

$$\dot{e_{x_1}} = A_{21}e_y + A_{22}e_{x_1} - L_2L_1^{-1}(L_1 sgn(e_y))_{eq} \tag{5.17}$$

The above equation with the insertion of (5.16), can be re-written as,

$$\dot{e_{x_1}} = A_{22}e_{x_1} - L_2L_1^{-1}A_{12}e_{x_1} \tag{5.18}$$

$$\implies \dot{e_{x_1}} = (A_{22} - L_2 L_1^{-1} A_{12}) e_{x_1} \tag{5.19}$$

It is assumed before that the couple of (A, C) is observable and this very assumption is sufficient to legitimatize that the pair $(A_{22}, A12)$ is also observable. The Eigen values of the matrix $(A_{22} - L_2 L_1^{-1})$ can be assigned randomly and this matrix determines the reconstruction speed, choosing the value of appropriately, the error will decay exponentially, consequently the observed states will converge to the actual states.

5.2.1 Sliding-mode Observer for the Grid Integrated PV Panel

The circuit configuration of the grid-integrated system is shown in the Figure 5.2.

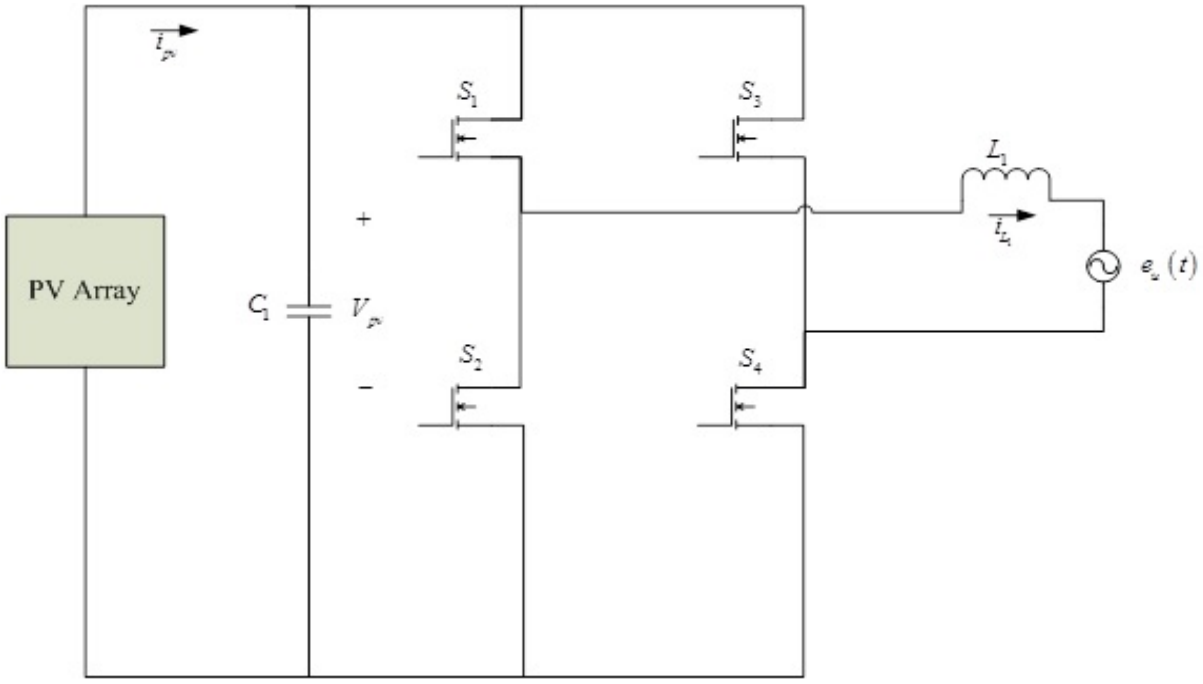

Figure 5.2: Single-phase grid connection of PV system

The system dynamics for the configuration can be obtained by applying KVL and KCL to the circuit. While writing the state equation we also introduce the modeling (parameter) uncertainties. At the instant when S_1 and S_4 are switched on whereas S_2 and S_3 are kept off,

$$\begin{aligned} \dot{v_{pv}} &= \frac{1}{C_1}(-i_{L_1} + i_{pv}) + \Delta f_u \\ \dot{i_{L_1}} &= \frac{1}{L_1}(v_{pv} - e_u(t)) \end{aligned} \tag{5.20}$$

when S_2 and S_3 are turned on and rest of the switches are not conducting then,

$$\begin{aligned} \dot{v_{pv}} &= \frac{1}{C_1}(i_{L_1} + i_{pv}) + \Delta f_u \\ \dot{i_{L_1}} &= \frac{1}{L_1}(v_{pv} - e_u(t)) \end{aligned} \tag{5.21}$$

Merging (5.20) and (5.21) the state space averaged model for the system can be deduced as,

$$\begin{aligned} \dot{v_{pv}} &= \frac{1}{C_1}(i_{L_1}.u + i_{pv}) + \Delta f_u \\ \dot{i_{L_1}} &= \frac{1}{L_1}(v_{pv}.u - e_u(t)) \end{aligned} \tag{5.22}$$

Where, v_{pv} is the voltage across C_1, i_{L_1} is the current through the inductor and $e_u(t)$ is the utility grid voltage. The term Δf_u depicts the uncertainties associated with measurement errors and modeling incurred due to the parameter variation from their nominal values. u represents the control input and acquire continuous values ranging from -1 to 1. As mentioned in the PV array modeling chapter the solar array current is a function of temperature, voltage and the light generated current I_{pv}. The current generated by the solar array i_{pv} can be defined as a state variable. It is necessary to measure the PV array voltage v_{pv} and the current flowing through the inductor i.e., i_{L_1} in order to track the MPP of the PV array. Synchronization of the phase in order to feed it to the utility is viable, only if we measure the utility grid voltage $e_u(t)$ and the current through the inductor i_{L_1} From the fig.5.2 and (5.22) it is clear that V_{pv} and i_{L_1} are measurable whereas, the PV array current i_{pv} is a function of the voltage across the capacitor C_1 and

the current flowing through the inductor. Hence,the current from the solar array i_{pv} can be observed or estimated from the measurable statesi_{L_1} and v_{pv}.

The ripple frequency of the voltage and current of the PV array is twice that of the grid frequency as the PV system is connected to grid. Relevantly the grid power, product of grid voltage and grid current also possess ripple components. Due this reason the MPPT controller takes the average values of PV array current and voltage to update the reference voltage instead of instantaneous value in order to mitigate erroneous readings. Hence, the estimated current is an average value. Based on the aforesaid average context, it allows us to assume that the derivative of the PV array current i_{pv} is equal to zero, regardless of the ripple components present in it if the sampling frequency is high enough compared to the solar array current dynamics. Considering these assumptions (5.22) takes the form,

$$\begin{aligned} \dot{v_{pv}} &= \frac{1}{C_1}(i_{L_1}.u + i_{pv}) + \Delta f_u \\ \dot{i_{pv}} &= 0 \\ y &= v_{pv} \end{aligned} \tag{5.23}$$

The associated sliding-mode based observer for (5.23) is presented as [14],

$$\begin{aligned} \dot{\hat{v_{pv}}} &= \frac{1}{C_1}(-i_L.u + \hat{i_{pv}}) + L_A sgn(e_y) \\ \dot{\hat{i_{pv}}} &= L_B(L_A sgn(e_y)) \\ e_y &= y - \hat{y} = v_{pv} - \hat{v_{pv}} \end{aligned} \tag{5.24}$$

$$sgn(e_y) = \begin{cases} +1 & e_y > 0 \\ -1 & e_y < 0 \end{cases}$$

Here $\hat{v_{pv}}$ and $\hat{i_{pv}}$ are the observed or estimated values of v_{pv} and i_{pv}.L_A and L_B are the observer gains. The current error ids defined as $e_i = i_{pv} - \hat{i_{pv}}$. Therefore, the error dynamics obtained are,

$$\dot{e_y} = \frac{e_i}{C_1} + \Delta f_u - L_A sgn(e_y) \tag{5.25}$$

$$\dot{e_i} = -L_B L_A sgn(e_y) \tag{5.26}$$

By choosing a substantial value of L_A, it is guaranteed that both e_y and $\dot{e_y}$ will have different signs. For a provided value of L_A, the following condition holds for the error dynamics.

$$\begin{aligned} e_y > 0 : \dot{e_y} &= \frac{e_i}{C_1} + \Delta f_u - L_A \implies \dot{e_y} < 0 \\ e_y < 0 : \dot{e_y} &= \frac{e_i}{C_1} + \Delta f_u + L_A \implies \dot{e_y} > 0 \end{aligned} \tag{5.27}$$

From (5.27) it is clear that the underneath inequality is satisfied:

$$e_y.\dot{e_y} < 0 \tag{5.28}$$

Hence, the output error diminishes to zero. It is a concerned objective while designing an appropriate observer based on sliding-mode theory to select a sliding manifold. For the proposed configuration sliding mode appears on the manifold of output error. According to the method of equivalent control method briefed in the observer section, the sliding mode of the system acts in a manner as if $L_A sgn(e_y)$ were ousted by its equivalent value $(L_1 sgn(e_y))_e qv$, in order to get rid of the uncertainties in (5.25) it is assumed that $\dot{e_y} = 0$ when trajectory of sliding-mode is restricted on the sliding manifold i.e., $e_y = 0$. After the attainment of the sliding surface as per the equivalent control notion, e_y as well as $\dot{e_y}$ both decays to zero and the associated uncertainties disappear. Substituting $e_y = 0$ and $\dot{e_y} = 0$ in (5.25)results in,

$$L_A sgn(e_y)_{eqv} = \frac{e_i}{C_1} \tag{5.29}$$

substituting the above equation in (5.26) we get,

$$\dot{e_i} = -L_B.\frac{e_i}{C_1} \tag{5.30}$$

Thus, from (5.30) the ensuing current error inequality is always true,

$$\dot{e_i}.\dot{e_i} = -\frac{L_B}{C_1}.e_i^2 < 0 \tag{5.31}$$

Therefore, as long as the value of L_B is chosen to be a positive value the convergence condition of the current error is always fulfilled.

5.2.2 Average Values of estimated and actual PV array current

In order to avoid errors while tracking MPP of the solar array it had been already assumed that the tracking system uses the average current instead its instantaneous value, provided the switching frequency is high. It was also mention earlier in this writing that the current of the PV array oscillates at twice the grid frequency, here 100Hz (2×50) imposed due to the sinusoidal inductor current. It was also assumed in (5.23) that the derivative of the PV array current is equal to zero.As the array current itself contains ripple components, it is obvious that the current error e_i also contains ripple components. In order to eliminate these ripple components the average of current error over the half cycle of the grid frequency is considered. The following deduction leads to the derived legitimacy of the averages of estimated and actual values of the current.

$$\frac{1}{\frac{\tau}{2}} \int_0^{\frac{\tau}{2}} e_i.dt = 0 \tag{5.32}$$

$$\frac{1}{\frac{\tau}{2}} \int_0^{\frac{\tau}{2}} (i_{pv} - \hat{i_{pv}}).dt = 0$$

$$\frac{1}{\frac{\tau}{2}} \int_0^{\frac{\tau}{2}} i_{pv}.dt = \frac{1}{\frac{\tau}{2}} \int_0^{\frac{\tau}{2}} \hat{i_{pv}}.dt \tag{5.33}$$

$$\implies (i_{pv})_{avg} = (\hat{i_{pv}})_{avg}$$

Where, $\tau = \frac{1}{f}$ and $f = 50$ is the frequency of the grid. Therefore, the estimated average PV array current is equal to the average of the actual current which is supplied to the MPPT block in place of the actual PV array current. Like wise the average of the PV array voltage is fed to the tracking block.

5.2.3 Range of Observer Gain

The stability and magnitude of chattering is governed by the observer gains L_1 and L_2. Although sliding mode observer is known for its robustness against disturbances, it does have a limitation on this property. The sliding-mode based observer is developed by the equations of the system and the switching gains L_A and L_B can be assigned arbitrarily to achieve robustness in presence of disturbances. However,

the limitation associated with the observer gains comes in from the qualification that the observer is stable[22]. The range of L_A depends on the maximum value of the PV array current and the quantity of uncertainties. The estimation error of the PV array current is bounded by the product of number of cells connected in parallel and current generated by sunlight $N_p.I_{pv}$ and corresponds to the short circuit current of the PV array. It is already stated in the second chapter that the short circuit current depends on the temperature and insolation level. If the boundaries of insolation and temperature are known, then $N_p.I_{pv}$ determines the maximum value of the PV array current. The uncertainty Δf_u is bounded by a known value σ_1. The range of the observer gain L_B is therefore given as,

$$L_B > max(\frac{e_i}{C_1} + \Delta f_u) = |\frac{e_i}{C_1}| + |\Delta f_u| = \frac{N_p.I_{pv}}{C_1} + \sigma_1 \tag{5.34}$$

The overall controller configuration for the inverter is given below in Figure 5.3. The PLL (Phase lock loop) is used in order to match the phase of the injected current with the grid voltage. The PI controller takes the error of actual voltage of the solar array and the reference voltage generated by the MPPT system.

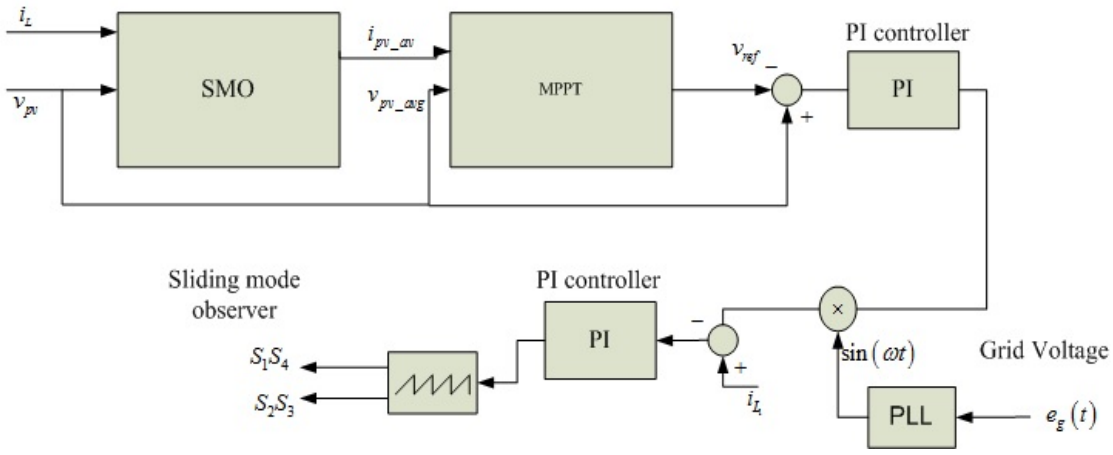

Figure 5.3: Overall Controller configuration

5.3 Simulation results with the SMO

The values of the parameters associated with the SMO and the inverter for performing the simulation are presented in table 5.1.

Table 5.1: Values of parameters for simulation

Capacitor, C_1	1000 μF
Inductor , L_1	5 mH
Observer gain, L_B	0.5
Observer gain, L_A	1000
Grid voltage	25 V_m, 50 Hz
Sampling frequency, f_s	10kHz

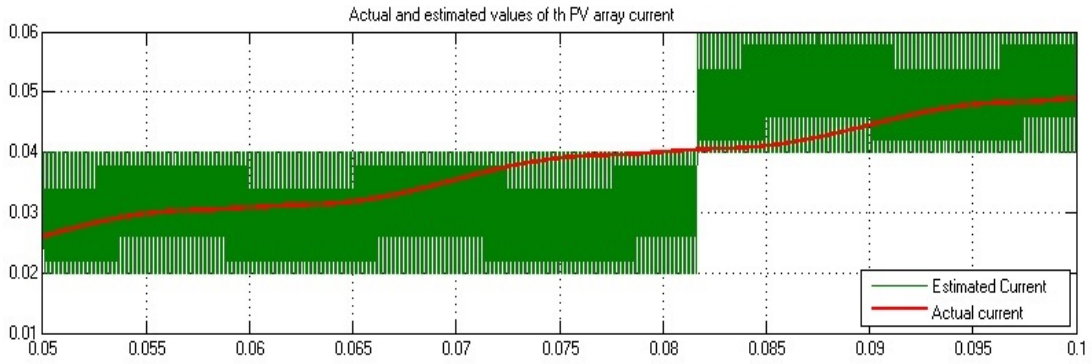

Figure 5.4: Estimated and actual state of PV array current

Fig 5.4 shows the estimated state of solar array current, for a capacitor value of $1000\mu F$ and $I_{pv=8.214}$ the value of L comes around 8000 from (5.34). The observer gain L_A takes a value of 0.5. It is already been stated in this chapter that the magnitude of chattering depends on the selection of observer gain in order to attain stability though they can be assigned with any random values but still restricted and this restriction is governed by (5.34).In Figure 5.4 we can see that the magnitude of chattering is high but sure is, following the actual current.

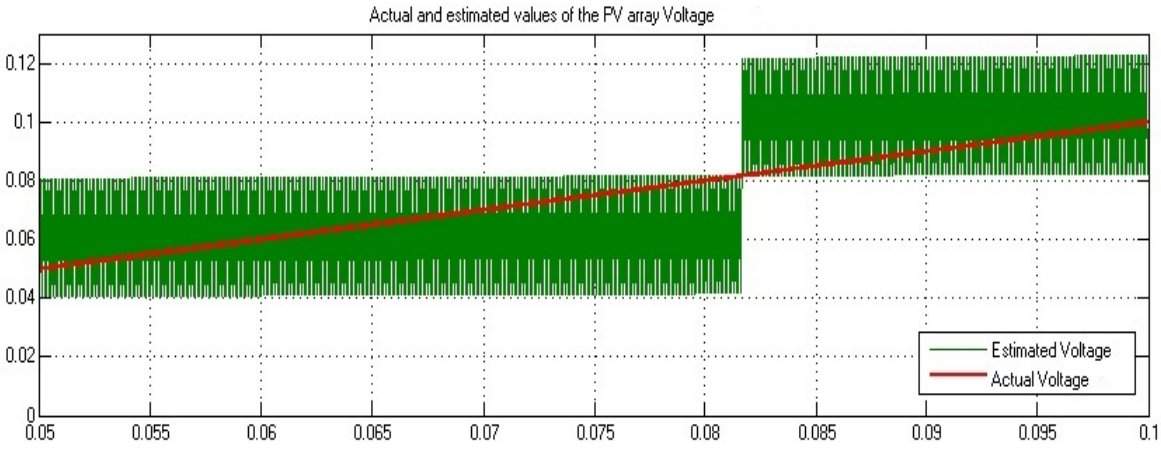

Figure 5.5: Estimated and state of PV array voltage

The estimated voltage and actual voltage is shown in Figure 5.5 for the same value of observer gains. The estimated voltage overlaps the actual value or rather we can say that it coincides the actual value. The chattering phenomena is also high in this case.

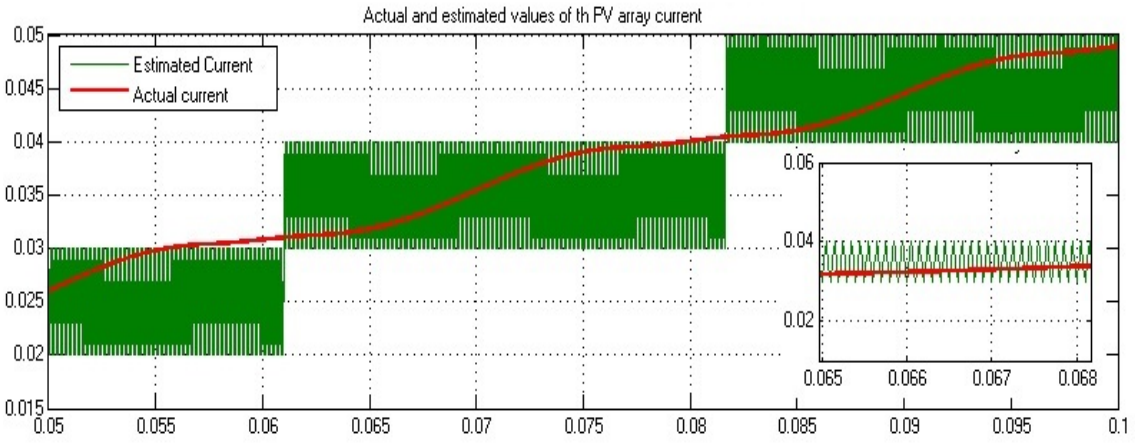

Figure 5.6: Estimated and actual state of PV array current,$L_A = 4000$

When the observer gain is adjusted to a newer value of $L_A = 4000$ the magnitude of chattering reduces and the estimation is more precise and follows the actual current as shown in Figure 5.6.

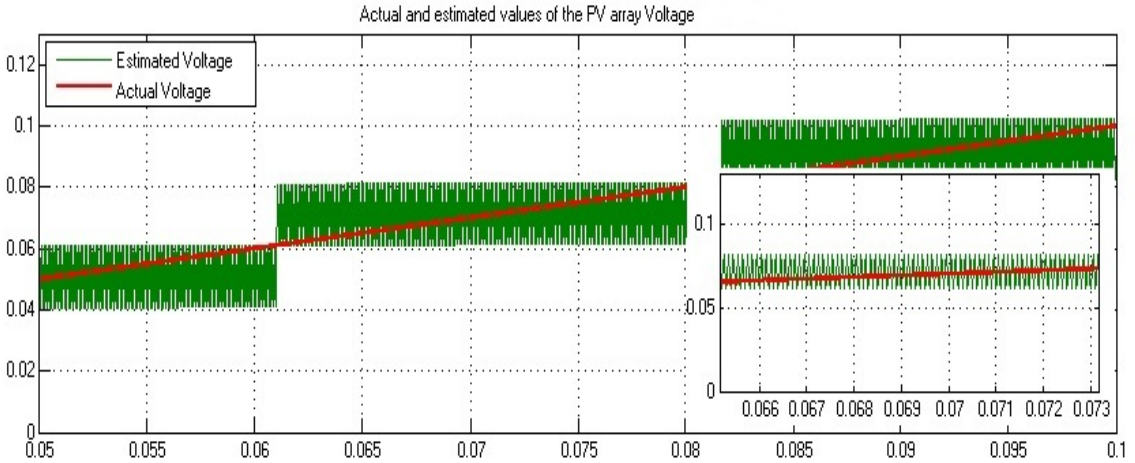

Figure 5.7: Estimated and state of PV array voltage,$L_A = 4000$

The chattering magnitude reduces to a much greater value i.e., almost two units and its clear from the figure that the estimated value follows the actual value of PV array voltage as in Figure 5.7.

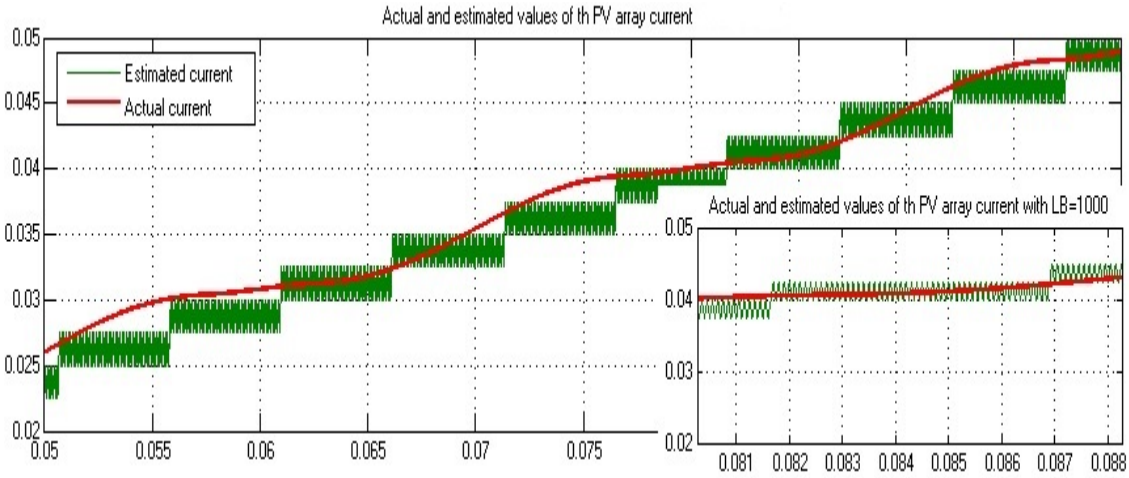

Figure 5.8: Estimated and actual state of PV array current,$L_A = 1000$

With observer gain value of $L_A = 1000$ the magnitude of chattering further reduces. The estimated current and real current are shown in Figure 5.8.

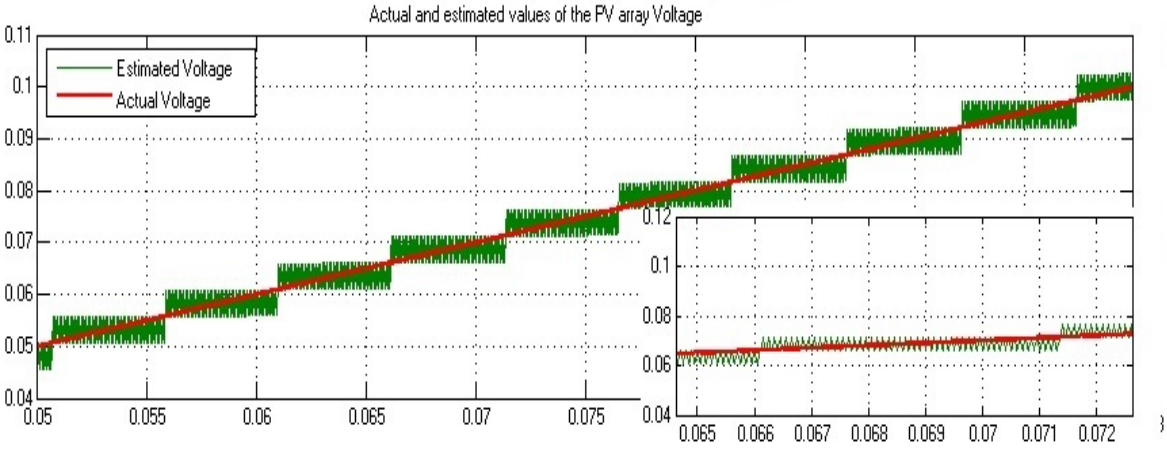

Figure 5.9: Estimated and state of PV array voltage,$L_A = 1000$

For the same value of L_A the estimated and actual value of the PV array voltage is shown in Figure 5.9.

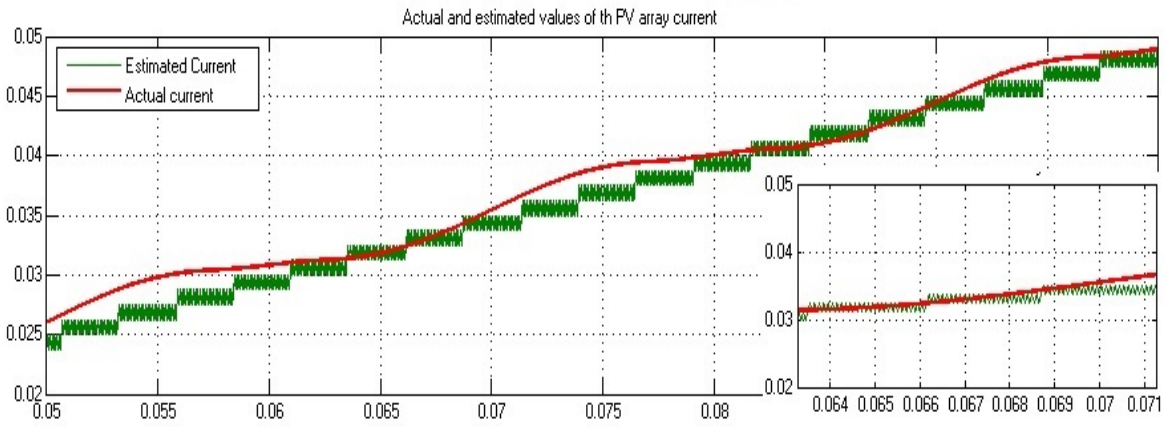

Figure 5.10: Estimated and actual state of PV array current,$L_A = 500$

If the value of the observer gain is further decreased, and from looking at the Figure 5.10 see that the estimation slightly deteriorates from the actual value. However, the chattering magnitude reduces to a much lower value but the observer is not stable as the estimation does not quite coincide with the actual value. So, choosing this value of observer gain would lead into erroneous operation.

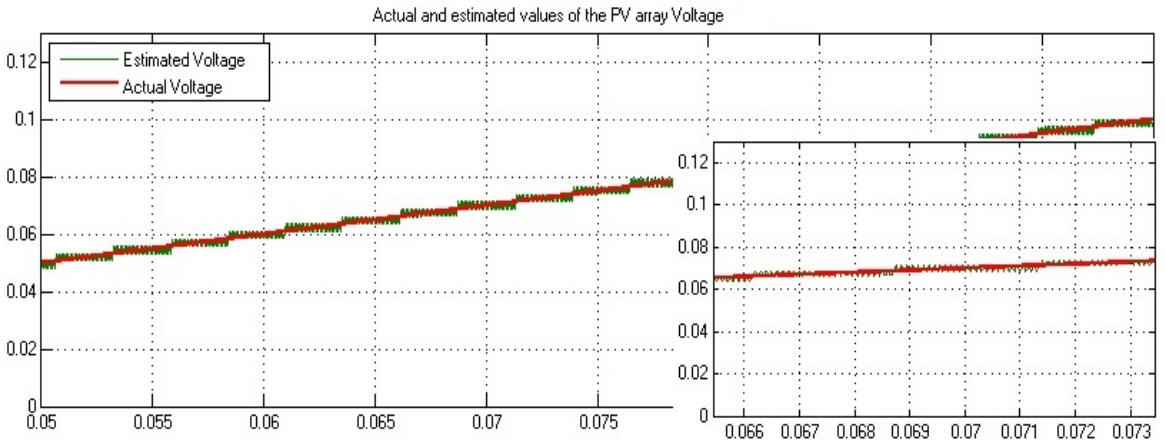

Figure 5.11: Estimated and actual state of PV array voltage,$L_A = 500$

The estimated value exactly coincides with the actual value of the voltage as can be seen from Figure 5.11. The chattering phenomena is almost in the vicinity of negligence but our concern is also with the current estimation, which denies the candidature of this value of observer gain. It can be inferred that choosing the value of the observer gain should be such a value for which the observer is stable and estimation coincides the actual value [22]. Here it is 1000.

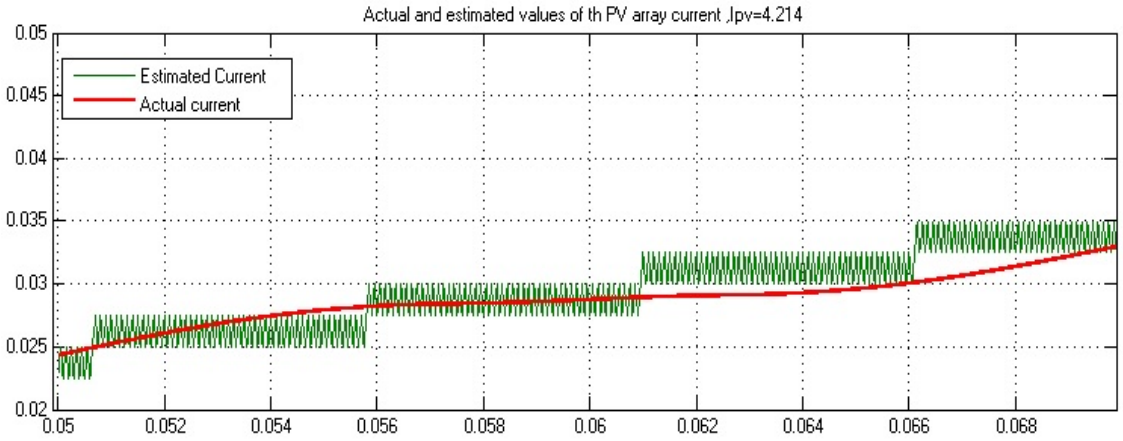

Figure 5.12: Estimated and actual state of PV array current,$I_{pv} = 4.124$

When it comes to checking the robustness of the sliding-mode observer it is done by varying the PV array current. For the Figure 5.12 the array current was lowered to a value of 4.214 and observer gain value $L_A = 1000$ it is seen that the estimation still follows the actual value which has decreased in magnitude due to the falling of solar array current.

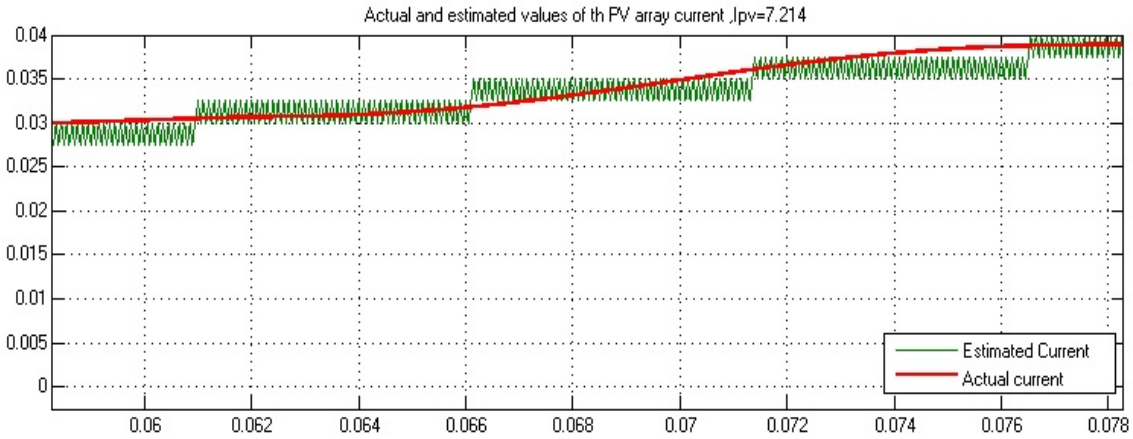

Figure 5.13: Estimated and actual state of PV array current,$I_{pv} = 7.124$

When the solar array current is set for 7.214 the magnitude of the actual voltage slightly reduces but the estimated value still follows the actual voltage regardless of the changes in solar array current. Thus,once again it is proved that the sliding-mode observer is robust against disturbances and this is shown in Figure 5.13.

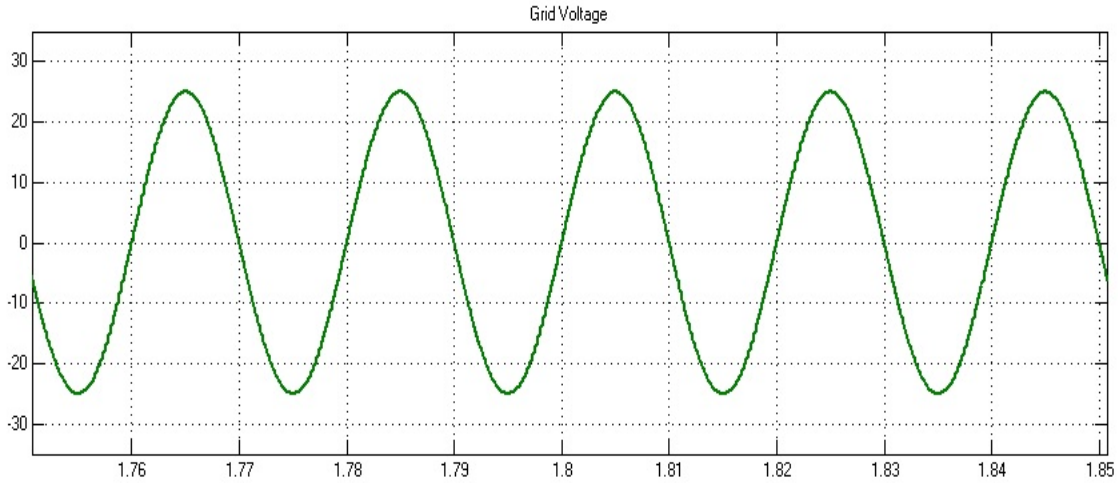

Figure 5.14: Grid side voltage

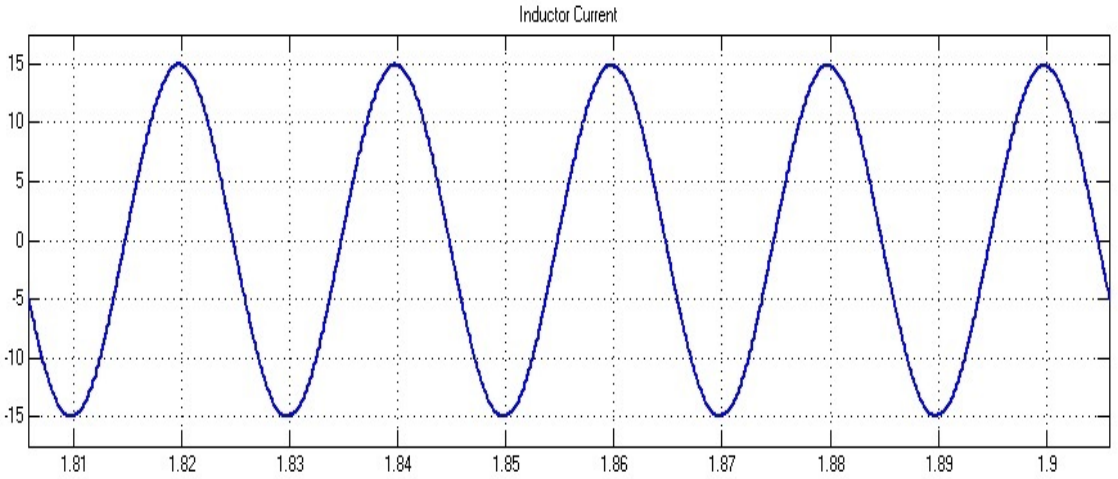

Figure 5.15: inductor current

The grid voltage is set to a peak value of 25 and has a frequency of $50Hz$. The grid voltage and inductor current obtained are shown in the Figure 5.14 and Figure 5.15. Thus, the estimation is performed and the grid integration of the PV array was done with grid.

Chapter 6

Conclusion and Scope for Future

Chapter 6

Conclusion and Future scope

6.1 Conclusion

The current estimation of the PV array current has been done using a sliding mode observer, which was constructed from the dynamics of the grid connected PV system. The average value of the estimated current was fed along with the array voltage to the MPP tracker, which generates a reference signal and was utilized to generate control signals for the inverter. It was also deduced that the average values of the estimated and actual current are equal.

A PV array of suitable ratings along with an H-bride inverter and a filter inductor was connected to the grid for performing simulations. Various waveforms with variations has been obtained to legitimatize the robust nature of the sliding mode observer.The average value of estimated current over half cycle of the grid voltage coincide with the actual value.

6.2 Suggestions for future

In the present system the voltage generated by the PV array has not been boosted which is of great concern for low voltage PV modules. The estimation of current after incorporating a dc-dc converter will of course sack the current sensor expenses but will also provide a better option for modular configuration, as this topology is widely used nowadays. Implementation of a more precise PLL transformation will improve the synchronization of the grid voltage and inductor current. The

use of the Inductor filter is a conventional way of filtering the harmonics, an LCL filter designed for the system would further enhance the voltage and current to be injected into the grid.

Bibliography

[1] McDonald, John D., et al. "Distribution Systems, Substations, and Integration of Distributed Generation." *Electrical Transmission Systems and Smart Grids*, Springer New York, 2013. 7-68

[2] Anees, Ahmed Sharique. "Grid integration of renewable energy sources: Challenges, issues and possible solutions." *2012 IEEE 5th India International Conference on Power Electronics (IICPE)*.2012.

[3] Coster, Edward J., et al. "Integration issues of distributed generation in distribution grids." *Proceedings of the IEEE*99.1 (2011): 28-39.

[4] Villalva, Marcelo Gradella, and Jonas Rafael Gazoli. "Modeling and circuit-based simulation of photovoltaic arrays." *Power Electronics Conference, 2009. COBEP'09. Brazilian.*IEEE, 2009.

[5] Villalva, Marcelo Gradella, and Jonas Rafael Gazoli. "Comprehensive approach to modeling and simulation of photovoltaic arrays." *IEEE Transactions on* 24.5 (2009): 1198-1208.

[6] Adaval, G. Spagnuolo, LG Franquelo, CA Ramos-Paja, T. Suntio, WM Xiao, "Grid-connected photovoltaic generation plants," *IEEE Industrial Electronics Magazine*,Sep 2013

[7] Esram, Trishan, and Patrick L. Chapman. "Comparison of photovoltaic array maximum power point tracking techniques." *IEEE Transactions on energy conversion EC 22.2*(2007): 439.

[8] Patil Sahebrao, N., and R. C. Prasad. "Design and simulation of MPPT algorithm for solar energy system using Simulink model." (2014).

[9] Sahu, Tekeshwar Prasad, T. V. Dixit, and Ramesh Kumar. "Simulation and Analysis of Perturb and Observe MPPT Algorithm for PV Array Using CUK Converter."

[10] Liu, Fangrui, et al. "Comparison of $P\&O$ and hill climbing MPPT methods for grid-connected PV converter." *Industrial Electronics and Applications, 2008. ICIEA 2008. 3rd IEEE Conference on.*IEEE, 2008.

[11] Patel, Hiren, and Vivek Agarwal. "A single-stage single-phase transformer-less doubly grounded grid-connected PV interface." *IEEE Transactions on* 24.1 (2009): 93-101.

[12] Jain, Sachin, and Vivek Agarwal. "A single-stage grid connected inverter topology for solar PV systems with maximum power point tracking." *Power Electronics, IEEE Transactions on* 22.5 (2007): 1928-1940.

[13] Edwards, Christopher, Leonid Fridman, and Arie Levant. "Sliding mode control and observation" Birkhuser, 2014.

[14] Haskara, Ibrahim, Umit Ozguner, and Vadim Utkin. "On variable structure observers." *Variable Structure Systems, 1996. VSS'96. Proceedings. 1996 IEEE International Workshop on*IEEE, 1996.

[15] Sim-Ramirez, Hebertt. "A Sliding Mode Controller-Observer for DC-toDC Power Converters: A Passivity Approach." (1995).

[16] Kjaer, Soeren Baekhoej, John K. Pedersen, and Frede Blaabjerg. "A review of single-phase grid-connected inverters for photovoltaic modules." *IEEE Transactions on* 41.5 (2005): 1292-1306.

[17] Ciobotaru Mihai, Remus Teodorescu, and Frede Blaabjerg, "Control of single-stage single-phase PV inverter," *European Conference on Power Electronics and Applications, IEEE*,2005.

[18] Kjaer, Soeren Baekhoej, John K. Pedersen, and Frede Blaabjerg,"A review of single-phase grid-connected inverters for photovoltaic modules," *IEEE Transactions on Industry Applications*, 41.5 (2005): 1292-1306.

[19] Amakye Dickson, N Mensah Sitti, Daniel Owusu Donkor, Nina PearlDoe and Ernest A. Amakye,"Grid Connected Inverters with unity Power Factor Renewable Energy (PV) Application," *International Journal of Innovative Science, Engineering & Technology*, Vol. 1 Issue 3, May 2014.

[20] Hashimoto, Hideki, V. I. Utkin, Jian-Xin Xu, Hiroyuki Suzuki, and Fumio Harashima,"Vss observer for linear time varying system," *Industrial Electronics Society, 16th Annual Conference of IEEE*, (1990):34-39.

[21] V.L. Utkin,"Sliding Modes and Their Application in Variable Structure Systems,"Imported Publication Incorporated, 1978.

[22] Y. J., C. C. Chan, and K. T. Chau."A novel sliding-mode observer for indirect position sensing of switched reluctance motor drives." *Industrial Electronics, IEEE Transactions on*, 46.2 (1999): 390-397.